# FALCON: a functional atlas of language comprehension networks based on multiple task-induced activation mapping and graph analysis of intrinsic connectivity in 137 healthy right-handers

Labache L[1,2,3,4,5], Joliot M[1,2,3], Saracco J[4,5], Jobard G[1,2,3], Hesling I L[1,2,3], Zago L[1,2,3], Mellet E[1,2,3], Petit L[1,2,3], Crivello F[1,2,3], Mazoyer B[1,2,3], Tzourio-Mazoyer N[1,2,3]

**Abstract** We herein propose an atlas of 32 language-related areas based on a 3-step method combining the analysis of activation and asymmetry during multiple language tasks with hierarchical clustering of resting-state connectivity and graph analyses. In total, 144 healthy right-handers performed fMRI runs based on language production, reading and listening, both with sentences and lists of over-learned words. Sentence minus word-list BOLD contrast and left-minus-right BOLD asymmetry for each language task were computed in pairs of homotopic regions of interest (hROIs) from the AICHA atlas. Thirty-two hROIs were identified that were conjointly activated and leftward asymmetrical in each of the 3 language contrasts. Analysis of resting-state temporal correlations of BOLD variations between these 32 hROIs allowed the segregation of four networks: LANG_CORE (including 16 hROIs of language-essential areas), LANG_EXE (including 4 hROIs involved in executive functions), LANG_VISU (composed of 5 hROIs belonging to visual cortices), and LANG_DMN (including 7 hROIs belonging to the default mode network (DMN)). At rest, LANG_CORE was positively correlated with LANG_EXE and negatively correlated with LANG_DMN. Graph analysis methods applied to LANG_CORE hROIs revealed that the pars triangularis region of the inferior frontal gyrus and 2 hROIs of the superior temporal sulcus were hubs based on their degree centrality (DC), betweenness and participation values. These core areas for intra- and inter-network communication correspond to the epicentres of sentence processing. Positive correlations between DC and BOLD activation strength values were observed in not only LANG_CORE hROIs across individuals but also across regions regardless of the language task, demonstrating that more connected areas have stronger activation responses. DC measurements in LAN_CORE may thus be a valuable index to evaluate inter-individual variations in language area activities in large populations in relation to anatomical and clinical patterns in language pathologies. The atlas comprising these 4 networks is named FALCON (Functional Atlas of Language COmprehension Networks) and can be downloaded at http://www.gin.cnrs.fr/en/tools/.

**Keywords** fMRI · Left hemisphere · Language production · Reading · Comprehension · Atlas · Intrinsic connectivity · Graph analysis · Right-handers

Corresponding author:

Nathalie Tzourio-Mazoyer

nathalie.tzourio-mazoyer@u-bordeaux.fr

[1] Univ. Bordeaux, IMN, UMR 5293, F-33000 Bordeaux, France

[2] CNRS, IMN, UMR 5293, F-33000 Bordeaux, France

[3] CEA, GIN, IMN, UMR 5293, F-33000 Bordeaux, France

[4] ENSC – Bordeaux INP, IMB, UMR 5251, F-33405 Talence, France

[5] INRIA Bordeaux Sud-Ouest, CQFD, INRIA, UMR 5251, F-33405 Talence, France

## Introduction

Defining language areas is a complex enterprise because of the numerous possible approaches currently available to identify language-related regions. The gold standard is to consider that language areas correspond to regions wherein lesions lead to aphasia. Even when limiting the definition of language areas to that of essential language areas, different identification methods exist that provide various kinds of information. Wada testing allows identification of the hemisphere controlling language but does not provide regional information (Wada & Rasmussen, 1960). By contrast, surgical cortical stimulation studies have documented left hemisphere language areas in large samples of patients (Ojemann, Ojemann, Lettich, & Berger, 1989; Tate, Herbet, Moritz-Gasser, Tate, & Duffau, 2014; Tate, Herbet, Moritz-Gasser, Tate, & Duffau, 2015), but such mapping of eloquent areas is still limited to the cortical regions available to the surgeon and is conducted in patients having potentially modified language organization. The probabilistic mapping of lesions combined with fine-grained aphasic patient evaluations of language performance have provided the community with very accurate descriptions of essential language areas (Dronkers & Ogar, 2004; Dronkers, Wilkins, Van Valin, Redfern, & Jaeger, 2004; Geva et al., 2011), although this very important approach does not reveal how these cortical areas are organized in networks. Because each multiple cortical area altered by a given pathology is not involved in the language deficit, the comprehensive identification of language

areas from lesions is a complex issue. Some researchers have used virtual lesions with transcranial magnetic stimulation (TMS) to access the regional organization of language (Ogar et al., 2006), but this approach limits the language functions tested, and the results are difficult to average across individuals.

Functional neuroimaging provides a way to map multiple areas activated during the completion of various language tasks in a large number of individuals. Furthermore, neuroimaging methodology is very efficient at compiling results obtained in multiple laboratories across the world, thereby allowing meta-analyses across laboratories that provide the location of areas activated at an acceptable spatial resolution within a common normalization space for a variety of language tasks (Vigneau et al., 2006). Similar to the results obtained with cortical stimulation (Ojemann et al., 1989), meta-analyses of neuroimaging data have provided the landscape of the left hemisphere cortical areas involved in language tasks in healthy individuals, which covers nearly the entire hemisphere surface (Price, 2000; Price, 2010; Price, 2012; Vigneau et al., 2006).

Despite the vast amount of information obtained from the methods cited above, an atlas of left hemisphere language areas in typically healthy individuals having a left hemisphere dominance for language is still lacking, and when referring to language areas, the absence of a consensus is blatant. The posterior part of the superior temporal gyrus and the supramarginal gyrus (Klingbeil, Wawrzyniak, Stockert, & Saur, 2017; Tomasi & Volkow, 2012) are phonological regions that can be found under the label «Wernicke's area», while lesion-based studies (Dronkers & Ogar, 2004; Pillay, Binder, Humphries, Gross, & Book, 2017; Yourganov, Smith, Fridriksson, & Rorden, 2015) as well as lesion studies in association with activation studies (Saur et al., 2006) have shown deep aphasia associated with the lesion of the posterior region of the middle temporal gyrus and superior temporal sulcus ((Binder, 2017; Binder, 2015)). There is more consistency concerning the location of frontal language areas under the label of Broca's area, because its original definition was anatomical. Most people defined Broca's area as the pars triangularis of the inferior frontal gyrus(Clos, Amunts, Laird, Fox, & Eickhoff, 2013; Friederici & Gierhan, 2013; Yourganov et al., 2015). However, the extent of Broca's area in the left frontal lobe varies, and the anterior insula (Baldo, Wilkins, Ogar, Willock, & Dronkers, 2011) is sometimes added, as reviewed in Amunts (Amunts & Zilles, 2012). Moreover, posterior lesions can also lead to Broca's aphasia (Richardson, Fillmore, Rorden, Lapointe, & Fridriksson, 2012), demonstrating that these anterior and posterior language poles work tightly together. This enhances the importance of networks in cognitive processing, as defined by Fuster (Fuster & Bressler, 2012). An atlas of language areas and networks in healthy individuals would thus be a useful tool, especially when individual task-induced mapping is not available. This atlas would be especially helpful for patients having difficulties completing language tasks and for the exploration of genetic language bases in large cohorts of individuals, in cohorts targeting normal or pathological brains, including those with developmental pathologies, and/or in individuals mapped for their anatomy and/or resting state while not performing a language task (Thompson et al., 2017).

To elaborate such an atlas, increasing the specificity for language areas that will be integrated is important because as uncovered by lesion studies, not all areas revealed by task-induced activation studies are essential language areas. Components of the task, such as monitoring, selecting, and holding the instructions, as well as paralinguistic processing, such as context, emotional and prosodic processing, are responsible for activations that exceed left hemisphere essential language areas. The strong right hemisphere activations observed with functional imaging during various language tasks have even led some authors to claim that neuroimaging methods are not adequate to map language regions (Sidtis, 2007). One way to overcome this issue is using appropriate reference tasks. To discriminate language areas among those involved in the completion of a given task, Binder has suggested using well-designed reference tasks. The idea is to remove the non-specific or non-lateralized activations of primary areas and/or executive regions by applying the difference paradigm (Binder, 2011). Compared to a non-verbal reference, the use of a verbal reference tasks allows left hemisphere language areas to be specifically highlighted, as shown by Ferstl's meta-analysis (Ferstl, Neumann, Bogler, & von Cramon, 2008). The use of verbal reference tasks with functional magnetic resonance imaging (fMRI) has proven to successfully measure asymmetric activations, a proxy of language dominance strongly concordant with Wada testing. Note that this is true when using both hemispheric and regional asymmetric activations (review in (Dym, Burns, Freeman, & Lipton, 2011)).

Thus, asymmetry represents an additional method for increasing the specificity of identifying left hemisphere language areas. Typical language organization, seen in more than 90% of the healthy population and in nearly all right-handers (Zago et al., 2017; Mazoyer et al., 2014), is characterized by a strong left hemisphere dominance, giving rise to regional leftward asymmetries in fMRI. Adding to the detection of activated areas (by comparison to a high-level verbal reference task), a criterion based on leftward asymmetry would certainly increase the specificity of identifying left hemisphere language areas.

Another difficulty in identifying essential language areas with functional imaging is the fact that different tasks lead to different patterns of activation. One way to overcome this difficulty is to combine several language tasks in the same participant and apply conjunction analyses to unravel the activated and asymmetrical regions independent of the type of task or modality involved (Papathanassiou et al., 2000; Jobard, Vigneau, Mazoyer, & Tzourio-Mazoyer, 2007; Dodoo-Schittko, Rosengarth, Doenitz, & Greenlee, 2012).

Finally, the task-induced approach does not provide any information on how the different activated areas are

organized in networks. The co-activation of a group of regions does not indicate that they are all strongly functionally connected and thus constitute a network. Resting-state intrinsic connectivity has proven to be capable of identifying the organization of brain network cognition. A good illustration of this concept is provided by Turken et al., who conducted correlation analysis in resting-state images of healthy participants using the posterior middle temporal gyrus region as the seed (Turken & Dronkers, 2011). In this work, this seed region was selected because its lesion was associated with strong comprehension deficits in aphasics, and its location was previously identified by probabilistic lesion mapping (Dronkers et al., 2004). Using this approach, Turken et al. revealed a network of areas connected at rest that support speech comprehension in healthy individuals. Investigating intrinsic connectivity would thus be an interesting means to investigate the networks existing at rest among the areas activated during language tasks. Connectivity measures can provide essential information on how regions are connected and how they are organized in networks. Graph analysis methodology applied on resting-state connectivity also permits the measurement of the connectivity strength of each region with all other regions of a given network to which it belongs, thereby characterizing its role in the network. In particular, identifying the topological roles of the regions is possible, i.e., identifying hubs, regions essential to a given network and therefore essential to the cognitive function(s) they support (Sporns, Honey, & Kötter, 2007).

To propose an atlas of left hemisphere high-order language areas, we first combined multiple language fMRI task-induced activation mapping and conjunction analysis to select a set of both activated and leftward asymmetrical areas. Second, we clustered the regions identified in the first step into networks based on their intrinsic connectivities at rest. Third, we applied graph analysis to characterize the roles of the regions in communication within and across networks. To do this, we utilized BIL&GIN, a database dedicated to the study of hemispheric specialization (Mazoyer et al., 2016), and selected 144 right-handers that were mapped during sentence production, reading and listening tasks compared to the production, reading and listening of lists of words, respectively. All but seven participants were also mapped during the resting state. Most investigations of the resting-state and task-induced activation networks have relied on whole-brain comparisons between the functional connectivities measured in these two conditions (review in Wig (Wig, 2017)), although they correspond to very different physiological states (Raichle & Mintun, 2006; Raichle, 2015). Here, we aimed to find resting-state markers of left hemisphere activation in discrete language areas to provide a comprehensive tool for further research on the inter-individual variability of language areas. Consequently, we used homotopical regions of interest (hROIs) from the AICHA atlas, a functional atlas obtained from intrinsic connectivity analysis (Joliot, Jobard, Naveau, Delcroix, & Petit…, 2015). The different sets of hROIs corresponding to the language areas of the proposed atlas are available in the Montreal Neurological Institute (MNI) space at http://www.gin.cnrs.fr/en/tools/.

## Material and methods

### Participants

From the BIL&GIN database, we selected 144 healthy right-handers (72 women) who completed the fMRI battery, including several language tasks (Mazoyer et al., 2016). The sample mean age was 27 years (SD = 6 years), and the women were two years younger than the men (women 26 ± 5; men: 28 ± 7, $p = 0.053$). The mean educational level of the participants was 16 years (SD = 6 years), with no significant difference between the men and women ($p > 0.05$). All participants reported themselves as right-handed; their mean normalized finger tapping test asymmetry ([(right number of taps - left number of taps) / (left + right number of taps)] x 100) was 6.25 (SD = 4.3), and their mean Edinburgh score was 93.5 (SD = 11), confirming their right-handedness. There was no difference between gender for the Edinburgh score ($p = 0.47$), although there was a slightly stronger rightward manual laterality in women (finger tapping test asymmetry in women: 6.9 ± 3.8; men: 5.7 ± 4.7, $p = 0.08$, controlling for age).

Of these participants, 137 (mean age 27 years (SD = 6 years), 68 women) also completed a resting-state fMRI (rs-fMRI) acquisition lasting 8 minutes. Note that this resting-state acquisition was performed on average 9 months (SD = 9.6 months) before the language task acquisition in all but 5 cases. In these 5 cases the resting-state acquisition occurred approximately one year after the language session (range [11.2 - 13.8] months).

### Image acquisition and processing

#### *Structural imaging*

Structural images were acquired using the same 3T Philips Intera Achieva scanner. High-resolution T1-weighted images were obtained using a 3D-FFE-TFE sequence (TR, 20 ms; TE, 4.6 ms; flip angle, 10°; inversion time, 800 ms; turbo field echo factor, 65; sense factor, 2; field of view, 256 × 256 × 180 mm3; isotropic voxel, 1 × 1 × 1 mm3). For each participant, the line between the anterior (AC) and posterior (PC) commissures was identified on a mid-sagittal section, and the T1-MRI volume was acquired after orienting the brain in the bi-commissural coordinate system. T2*-weighted multi-slice images were also acquired (T2*-weighted fast field echo (T2*-FFE), sequence parameters: TR = 3,500 ms; TE = 35 ms; flip angle = 90°; sense factor = 2; 70 axial slices; 2 x 2 x 2 mm3 isotropic voxel size).

### *Task-induced functional imaging*

*Training*

To ensure proper task execution, the participants were trained outside the scanner in the hour preceding the fMRI session. The training used stimuli that were of the same nature but different from those used during the fMRI session.

*Language tasks*

Three runs were administered to the participants. They included a sentence task involving phonological, semantic, prosodic and syntactic processing and a word-list reference task, a less complex, albeit high-level, verbal task. To achieve homogeneity in the sentence task material, 51 line drawings illustrating the stories of 'Le petit Nicolas' (Little Nicholas), a classic French children's series, were used. The three tasks consisted of a randomized alternation of event-related trials devoted to sentence processing, with event-related trials devoted to the verbal reference task, i.e., lists of words. The drawings used for the reference task were scrambled versions of the line drawings, and the stimuli presented either orally or visually were lists of months, days and/or seasons. Within each trial, the subject was shown either a line drawing or a scrambled drawing for 1 s, immediately followed by a central fixation crosshair. While fixating the cross, the subject performed either the sentence task or the word reference task. Once the task was completed, a low-level reference task, detecting the transformation of a centrally displayed cross into a square, was presented. When the subjects detected this change, they were asked to press a button with their index finger of the assigned hand. The square was then displayed until the end of the trial. This second part of the trial, which lasted at least half of the total trial duration, aimed at refocusing the subject's attention to a non-verbal stimulus and controlling for manual motor response activation, which was also present in the first part of the trial. A 12-s presentation of a fixation crosshair preceded and followed the first and last trial. Note that except during the drawings display, the subjects were asked to keep fixating the cross, and the star and square were then presented on the centre of the screen.

*Sentence and list of word production tasks* During the production run, after seeing a Little Nicholas line drawing, the subject was instructed to covertly generate a sentence beginning with a subject (The little Nicholas…, The gentleman…) and a complement (with his satchel…, in shorts…, with glasses…), followed by a verb describing the action taking place and ending with an additional complement of a place (in the street…, in the playground…, on the beach…) or a manner (with happiness…, nastily…). When a scrambled drawing was displayed, the subject was asked to covertly generate the list of the months of the year. The production paradigm randomly alternated ten 18-s trials of sentence generation with ten 18-s trials of generating the list of months. The response time limit, indicated by the transformation of the cross in a star, was 9 s, including the 1-s drawing display. The entire experimental run lasted 6 min and 24 s. The mean sentence production time was 5,617 ms (SD = 935 ms), while the mean duration of word-list production was 5,249 ms (SD = 1,131).

*Sentence and list of word listening tasks* When a Little Nicholas line drawing was displayed, the subject was instructed to carefully listen to a sentence dealing with the line drawing and click at the end of the sentence. For the LIST, when a scrambled drawing was displayed, he/she was instructed to listen to the list of the months, days of the week and/or seasons and click at the end of the list.

The paradigm consisted of a randomized alternation of thirteen 14-s sentence listening trials with thirteen 14-s list listening trials. The mean durations of auditory presentation were 4,371 ± 468 ms for the sentences and 4,386 ± 484 ms for the lists. The entire experimental run lasted 6 min and 28 s. The reaction times after sentence and list listening were 387 ms (SD = 125) and 478 ms (SD = 97), respectively.

*Sentence and list of word reading tasks* Like in the other two tasks, when a line drawing was displayed, the subject was instructed to read a sentence based on the line drawing. When a scrambled drawing was displayed, he/she was instructed to read the list of months, days of the week and/or seasons.

The paradigm consisted of a randomized alternation of thirteen 14-s sentence reading trials with thirteen 14-s list reading trials. The entire experimental run lasted 6 min and 28 s. The average time for reading sentences was 3,729 ms (SD = 567), while reading the lists of words required 4,412 ms (SD = 602).

*Debriefing the fMRI tasks*

Right after the fMRI sessions, the participants were asked to rate the difficulty of the task on a 5-point scale (1-easy to 5-very difficult) and answer some debriefing questions about how they accomplished the task.

The production task had the highest task difficulty score reported by the participants (2.73), while the reading and listening tasks had low scores (1.14 and 1.20, respectively). All participants were able to recollect the sentence they produced when presented with the corresponding drawing for at least 5 of 10 images (mean: 9.43, SD: 0.96), with the mean number of words per sentence being 12.4 (SD = 2).

### *Functional image acquisition*

The functional volumes were acquired as T2*-weighted echo-planar EPI images (TR = 2 s; TE = 35 ms; flip angle = 80°; 31 axial slices with a 240 x 240 mm2 field of view and 3.75 x 3.75 x 3.75 mm3 isotropic voxel size). In the

three runs, 192, 194 and 194 T2*-weighted volumes were acquired for the production, listening and reading sentence tasks, respectively.

***Resting-state functional imaging (rs-fMRI)***

Spontaneous brain activity was monitored for 8 minutes (240 volumes) using the same imaging sequence (T2*-weighted echo-planar images) as that used for the language tasks. Immediately prior to rs-fMRI scanning, the participants were instructed to "keep their eyes closed, to relax, to refrain from moving, to stay awake and to let their thoughts come and go".

***Image analysis***

*Functional imaging analysis common to task-induced and resting-state acquisitions*

For each participant, (1) the T2*-FFE volume was rigidly registered to the T1-MRI; (2) the T1-MRI was segmented into three brain tissue classes (grey matter, white matter, and cerebrospinal fluid; and (3) the T1-MRI scans were normalized to the BIL&GIN template (aligned to the MNI space), including 80 volunteers from the BIL&GIN database gender-matched using the SPM5 "segment" procedure with otherwise default parameters.

For each of the 3 fMRI runs, data were corrected for slice timing differences. To correct for subject motion during the runs, all the T2*-weighted volumes were realigned using a 6-parameter rigid-body registration. The EPI-BOLD scans were then registered rigidly to the structural T2*-FFE image. The combination of all registration matrices allowed for warping the EPI-BOLD functional scans to the standard space with a single trilinear interpolation.

*Specific task-induced functional imaging analysis*

First, a 6-mm full width at half maximum (FWHM) Gaussian filter was applied to each run. Global linear modelling (statistical parametric mapping (SPM), http://www.fil.ion.ucl.ac.uk/spm/) was used for processing the task-related fMRI data. For each participant, BOLD variations corresponding to each sentence versus the list belonging to the same run were computed (sentence minus word-list production ($PROD_{SENT\text{-}WORD}$), sentence minus word-list reading ($READ_{SENT\text{-}WORD}$), and sentence minus word-list listening ($LIST_{SENT\text{-}WORD}$)). Finally, contrast maps (defined at the voxel level) were subjected to ROI analysis. BOLD signal variations were measured in 192 pairs of functionally defined hROIs of the AICHA atlas (Joliot et al., 2015), excluding 8 hROI pairs belonging to the orbital and inferior-temporal parts of the brain in which signals were reduced due to susceptibility artefacts. For each participant, we computed contrast maps of the 3 language conditions. We then calculated the right and left hROI BOLD signal variations for each of the 184 remaining pairs by averaging the contrast BOLD values of all voxels located within the hROI volume.

*Specific analysis of resting-state functional images*

Time series for white matter and cerebrospinal fluid (individual average time series of voxels that belonged to each tissue class) and temporal linear trends were removed from the rs-fMRI data series using regression analysis. Additionally, rs-fMRI data were temporally filtered using a least squares linear-phase finite impulse response (FIR) filter design bandpass (0.01 Hz – 0.1 Hz).

For each participant and hROI (the same 184 homotopic ROIs as those used in the task-induced analysis), an individual BOLD rs-fMRI time series was computed by averaging the BOLD fMRI time series of all voxels located within the hROI volume.

| | L activation | L asymmetry | Conjunction of activation & asymmetry |
|---|---|---|---|
| $PROD_{SENT\text{-}WORD}$ | 138 | 92 | 80 |
| $LIST_{SENT\text{-}WORD}$ | 116 | 73 | 57 |
| $READ_{SENT\text{-}WORD}$ | 99 | 59 | 41 |
| Conjunctions of 3 contrasts | 84 | 46 | 32 |

**Table 1** Results of conjunction analyses across each sentence minus word-list contrasts for production (PRODSENT-WORD), listening (LISTSENT-WORD) and reading (READSENT-WORD) tasks in terms of the number of hROIs. Numbers of hROIs with significant left activation, leftward asymmetry or conjunction of activation and asymmetry for the 3 "sentence minus word" contrasts.

## Part 1. Identification and characterization of hROIs exhibiting both leftward activation and leftward asymmetrical activation in all 3 tasks

To complete the identification of high-order language areas, we first searched for hROIs that were both significantly co-activated and significantly leftward asymmetrical on average among the 144 participants during the $PROD_{SENT\text{-}WORD}$, $READ_{SENT\text{-}WORD}$, and $LIST_{SENT\text{-}WORD}$ tasks.

### Statistical analysis

Using JMP13 (www.jmp.com, SAS Institute Inc., 2012), conjunction analysis was conducted to select the left-hemisphere hROIs exhibiting BOLD signal variations that were both significantly positive and significantly larger than that in their right counterparts in all 3 tasks. The significance threshold was set to $p < 0.05$ for both activation and asymmetry, meaning that the significance threshold for the conjunction analysis was 1.5x10-8 per hROI.

### Results

Among the 84 hROIs jointly activated in the 3 contrasts

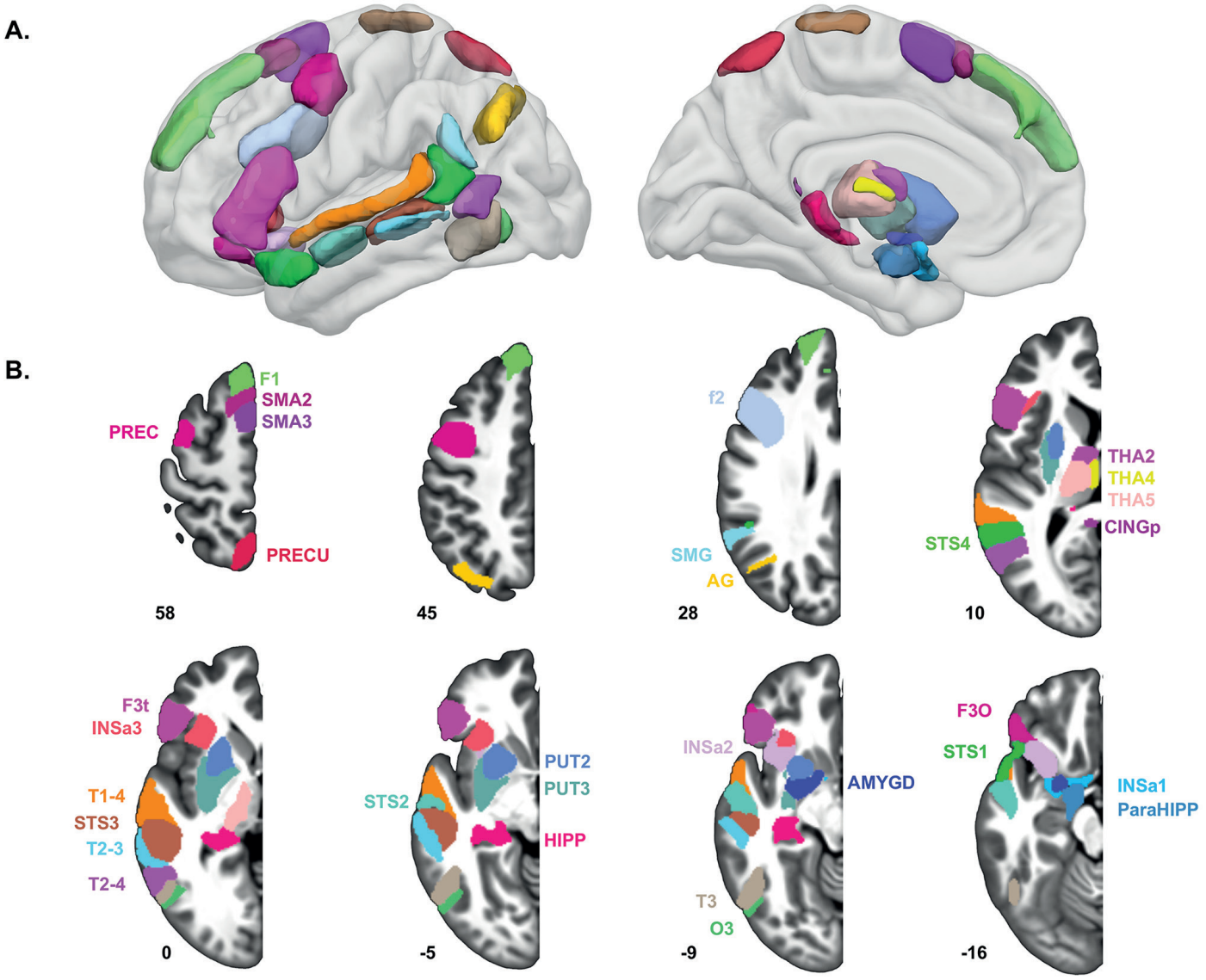


**Fig. 1** Locations of the 32 hROIs co-leftward activated and co-leftward asymmetrical during the completion of 3 sentence minus word-list tasks by 144 healthy right-handers. **a** Left lateral view of 3D surfaces rendering the hROIs on the BIL&GIN template in the MNI space with Surf Ice (https://www.nitrc.org/projects/surfice/) software. **b** Representation of hROIs on left hemisphere axial slices from the BIL&GIN template; the hROI numbers correspond to the z-axis in the MNI space. Correspondences between the abbreviations and the full names of the AICHA atlas can be found in Table 2.

(Table 1), 46 also showed joint asymmetries. Finally, 32 hROIs showed both joint activation on the left and joint asymmetry (Figure 1, Table 2). On the lateral surface of the left frontal lobe, the regions having both joint activation and leftward asymmetry during the 3 language tasks covered the left inferior frontal gyrus (pars triangularis: F3t and pars opercularis: F3O), the adjacent inferior frontal sulcus (f2) and the middle frontal gyrus, including the middle frontal gyrus junction with the precentral gyrus (PREC). hROIs located in the anterior part of the medial wall included the posterior cingulum gyrus (CINGp), the upper paracentral gyrus (Paracentral), the pre-superior motor area (SMA2 and SMA3) and the medial part of the superior frontal gyrus (F1). Several hROIs were located at the anterior insula (INSa1, INSa2 and INSa3).

On the lateral surface of the temporal lobe, the hROIs overlapped the entire length of the superior temporal sulcus (STS2, STS3 and STS4), extending to the temporal pole anteriorly (STS1), to the superior temporal gyrus dorsally (T1-4), to the supramarginal (SMG) and angular gyri (AG) posteriorly and to the junction between the inferior temporal gyrus (T3) and the inferior occipital gyrus (O3), crossing the middle temporal gyrus (T2-3 and T2-4). Regions located within the hippocampus (HIPP), parahippocampal gyrus (ParaHIPP) and amygdala (AMYGD) were also part of the selected areas. In the posterior medial wall, the dorsal part of the precuneus (PRECU) was selected by this approach.

Sub-cortical areas jointly activated and leftward asymmetrical during the 3 tasks covered almost the entire putamen (PUT2 and PUT3) and thalamus (THA2, THA4 and THA5).

| | AICHA hROI name | Abbreviation | Cluster |
|---|---|---|---|
| *Frontal & insula* | S_Precentral-4 | PREC | LANG_CORE |
| | G_Frontal_Sup-2 | F1 | LANG_CORE |
| | S_Inf_Frontal-2 | f2 | LANG_CORE |
| | G_Frontal_Inf_Tri-1 | F3t | LANG_CORE |
| | G_Frontal_Inf_Orb-1 | F3O | LANG_CORE |
| | G_Insula-anterior-1 | INSa1 | LANG_VISU |
| | G_Insula-anterior-2 | INSa2 | LANG_CORE |
| | G_Insula-anterior-3 | INSa3 | LANG_EXE |
| *Temporal & parietal* | G_Temporal_Sup-4 | T1-4 | LANG_CORE |
| | G_Temporal_Mid-3 | T2-3 | LANG_CORE |
| | G_Temporal_Mid-4 | T2-4 | LANG_CORE |
| | G_Temporal_Inf-4 | T3 | LANG_VISU |
| | S_Sup_Temporal-1 | STS1 | LANG_CORE |
| | S_Sup_Temporal-2 | STS2 | LANG_CORE |
| | S_Sup_Temporal-3 | STS3 | LANG_CORE |
| | S_Sup_Temporal-4 | STS4 | LANG_CORE |
| | G_SupraMarginal-7 | SMG | LANG_CORE |
| | G_Angular-2 | AG | LANG_DMN |
| | G_Occipital_Inf-1 | O3 | LANG_VISU |
| | G_ParaHippocampal-1 | ParaHIPP | LANG_VISU |
| | G_Hippocampus-2 | HIPP | LANG_DMN |
| *Internal surface* | G_Supp_Motor_Area-2 | SMA2 | LANG_CORE |
| | G_Supp_Motor_Area-3 | SMA3 | LANG_CORE |
| | G_Paracentral_Lobule-4 | Paracentral | LANG_DMN |
| | G_Cingulum_Post-3 | CINGp | LANG_DMN |
| | G_Precuneus-6 | PRECU | LANG_DMN |
| *Sub-cortical* | N_Amygdala-1 | AMYGD | LANG_VISU |
| | N_Thalamus-2 | THA2 | LANG_DMN |
| | N_Thalamus-4 | THA4 | LANG_DMN |
| | N_Thalamus-5 | THA5 | LANG_EXE |
| | N_Putamen-2 | PUT2 | LANG_EXE |
| | N_Putamen-3 | PUT3 | LANG_EXE |

**Table 2** Names and abbreviations of the 32 hROIs showing joint left activation and left asymmetry during the three sentences minus word-list contrasts for production ($PROD_{SENT\text{-}WORD}$), listening ($LIST_{SENT\text{-}WORD}$) and reading ($READ_{SENT\text{-}WORD}$) tasks and the network label to which they were clustered.

## Part 2. Identification of networks based on the resting-state connectivity matrix of the 32 hrois co-activated and co-leftward asymmetrical during the 3 sentence minus word-list tasks

In a second step, we investigated the intrinsic functional organization of the 32 hROIs selected in the first step. We computed the intrinsic connectivity matrix between these 32 hROIs for the subsample of 137 right-handed participants who completed a resting-state acquisition. We completed a hierarchical clustering analysis of this intrinsic connectivity matrix to identify temporally coherent networks within this set of hROIs.

## METHODS

### *Calculation of the intrinsic connectivity matrix*

An intrinsic connectivity matrix was calculated for each of the 137 individuals and for each of the 496 possible pairs of hROIs (N x (N-1))/2, with N = 32). The intrinsic connectivity matrix off-diagonal elements were the Pearson correlation coefficients between the rs-fMRI time series of the hROI pairs. The intrinsic connectivity matrix diagonal elements were set to zero because no information on the correlation for a specific hROI with itself exists (Rubinov & Sporns, 2010). The individual intrinsic connectivity matrix was then Fisher z-transformed before being averaged over the subsample of 137 individuals, thereby producing a mean intrinsic connectivity matrix.

### *Identification and characterization of networks*

The agglomerative hierarchical cluster analysis (aHCA) method was applied to extract brain sub-networks from this mean intrinsic connectivity matrix. The first step was to select a set of features describing each hROI. To do this, we used the mean intrinsic connectivity correlation value of a given hROI as the feature vector for assessing its temporal correlation with all other hROIs (31 correlation coefficients for each hROI). Next, we computed a dissimilarity

matrix using the Euclidean distance between each vector. Finally, we used the aHCA method to perform the clustering and the Ward distance to aggregate the different hROIs into clusters. We chose the number of networks based on the pseudo-T2 index value (as defined by Duda and Hart (Duda, Hart, & Stork, 2012)) provided by the R package "Nbclust" (Charrad, Ghazzali, Boiteau, Niknafs, & Charrad, 2014). Pseudo-T2 is specific to hierarchical clustering, as it corresponds to the within variance ratio after joining two clusters to the variance within each of the two aggregated clusters. A high Pseudo-T2 value indicates that the two joined clusters have highly different mean vectors.

To characterize each network, we calculated the mean voluminal activity for each task from the sum of the activations of ROIs composing the network weighted by their individual volumes and then divided by the sum of their total volume. We then calculated the left-minus-right asymmetries of the networks and compared the activation level and asymmetry values across networks (with ANOVA) and across tasks.

### *Reliability of the identified networks*

We used multiscale bootstrap resampling (Efron, Halloran, & Holmes, 1996) to assess the reliability of each cluster. In total, 10,000 multiscale bootstrap resampling datasets, including 50% to 140% of sample data from the 137 participants' (Suzuki & Shimodaira, 2004), were processed. Applying the R package "pvclust" (Suzuki & Shimodaira, 2006) function to the multiscale bootstrap resampling outputs, we measured the approximately unbiased (AU) p-value for each cluster. The AU p-value for a network, the probability of this network occurring among the 137 participants, indicates the network's reliability.

### *Robustness of the identified networks with respect to the clustering method*

We also assessed the robustness of the clustering method by comparing its output to those of 3 other clustering methods: aHCA with the average distance method (instead of Ward's), Gaussian mixture model, and k-Means (see supplementary material).

### *Temporal correlation across networks and significance*

To compute the mean intrinsic functional correlations between two networks, we used the same methodology as that used to compute the mean intrinsic connectivity matrix (see above). First, for each individual and for each network, we computed the corresponding rs-fMRI time series by averaging the individual resting time series of all voxels of all hROIs belonging to this network. Then, for each individual, we computed the Pearson correlation coefficients between all pairs of networks that we further Fisher z-transformed. Finally, each of these z-transformed coefficients was averaged across the sample of 137 individuals, providing a mean intrinsic functional correlation (r) for each pair of networks. We assessed the significance of each of these mean intrinsic functional correlations compared to 0 using a non-parametric sign test at the 0.05 significance level (Bonferroni correction for the number of network's pairs).

## Results

### *Identification and characterization of networks*

Hierarchical clustering analysis revealed four networks from the selected set of 32 hROIs (Figure 2).

#### *LANG_CORE network*

The first network (Figure 3A and pink on Figure 3B), termed LANG_CORE, was composed of 16 hROIs and was the most distant from the 3 others in terms of inertia. LANG_CORE included all lateral hROIs of the frontal and temporal lobes as well as those of the medial regions of the left hemisphere (F1, SMA1 and SMA2).

LANG_CORE was the largest network in terms of volume, as it was 4 times bigger than LANG_EXE, 5 times bigger than LANG_DMN and 7.5 times bigger than LANG_VISU (Table 3).

LANG_CORE was characterized by a significantly high activation of $PROD_{SENT\text{-}WORD}$ (all $p < 10^{-4}$), followed by $READ_{SENT\text{-}WORD}$ and $LIST_{SENT\text{-}WORD}$ activations. In addition, LANG_CORE showed the strongest significant asymmetry during the $PROD_{SENT\text{-}WORD}$ task (all $p < 10^{-2}$), while there was no significant difference in asymmetry between $READ_{SENT\text{-}WORD}$ and $LIST_{SENT\text{-}WORD}$.

#### *LANG_EXE network*

The smallest network in terms of the number of regions but second in terms of volume (Table 3) was composed of 4 hROIs (PUT2, PUT3, INSa3, located in the anterior part of the insula, and THA5) corresponding to sub-cortical and anterior insula hROIs, known to be involved in executive functions (see discussion). Accordingly, we named this network "LANG_EXE" (Figure 3B).

LANG_EXE was activated more during the PRODSENT-WORD task than during the other two tasks (Table 3, all $p < 10^{-4}$), while there was no significant difference between $READ_{SENT\text{-}WORD}$ and $LIST_{SENT\text{-}WORD}$. Note that LANG_EXE showed the same level of leftward asymmetry during all 3 tasks (all $p > 10^{-1}$).

#### *LANG_VISU network*

LANG_VISU was the smallest network in terms of volume (Table 3), as it gathered 4 hROIs, including 3 from the visual system (T3 and O3), the AMYGD and INSa1 adjacent to the amygdala, and ParaHIPP (Figure 3B).

LANG_VISU was significantly more activated during the $PROD_{SENT\text{-}WORD}$ task than during $READ_{SENT\text{-}WORD}$

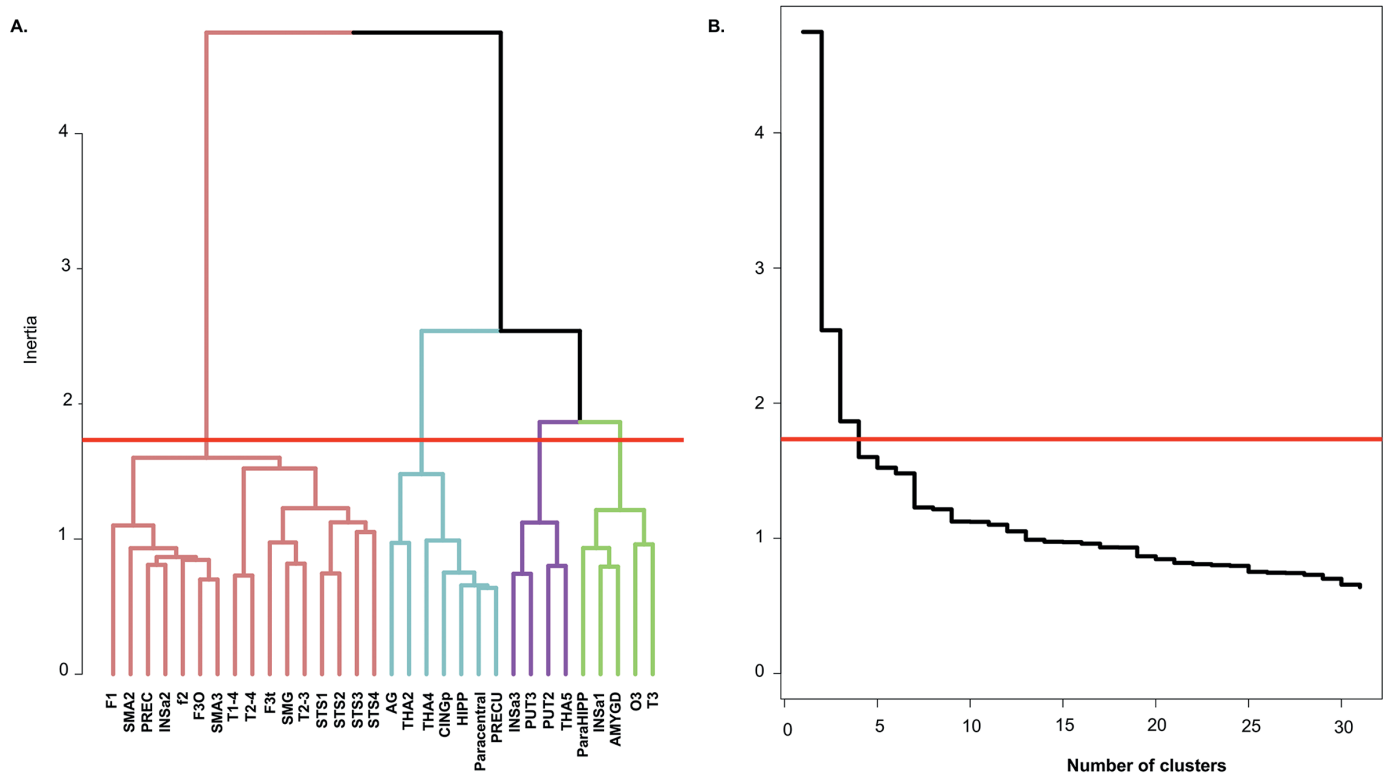


**Fig. 2** Results of the agglomerative hierarchical cluster analysis method. a Dendrogram of aHCA of the mean intrinsic connectivity matrix (LANG_CORE network: pink, LANG_DMN: light blue, LANG_EXE: purple, LANG_VISU: green). **b** Scree plot of aHCA of the mean intrinsic connectivity matrix. For both graphs, the red horizontal line corresponds to the threshold applied to select the number of sub-networks.

($p < 10^{-4}$, Table 3), while there was no significant difference between $PROD_{SENT\text{-}WORD}$ and $LIST_{SENT\text{-}WORD}$ ($p = 8.6.10^{-1}$) nor between $LIST_{SENT\text{-}WORD}$ and $READS_{ENT\text{-}WORD}$ ($p = 2.8.10^{-1}$). Finally, the 3 contrasts had comparable leftward asymmetries.

*LANG_DMN network*

The last sub-network was composed of 7 hROIs, including AG, PRECU, CINGp and HIPP, that belong to the default mode network (DMN) (Mazoyer, Zago, Mellet, Bricogne, & Etard…, 2001; Raichle, 2015), plus 2 hROIs located in the thalamus: THA2 (antero-dorsal part) and THA4 (medial part) (Figure 3B).

In terms of mean activation (Table 3), LANG_DMN had the same activation pattern as LANG_VISU; it was most activated during the $PROD_{SENT\text{-}WORD}$ task (all p < 10-4), and there was no significant difference between $LIST_{SENT\text{-}WORD}$ and $READ_{SENT\text{-}WORD}$. There were no significant differences in leftward asymmetry among the three tasks ($p > 3.10^{-1}$).

***Profile comparisons between networks***

In terms of mean voluminal activity (Table 3), ANOVA revealed a significant network effect, a task effect and a network x task interaction (all post hoc Tukey's HSD: $p < 10^{-4}$).

This interaction was because LANG_CORE was both the most activated and the most leftward asymmetrical network (Table 3) for the 3 tasks (all $p < 5.10^{-3}$). Furthermore, this interaction was also due to the significant difference between the DMN and VISU activations ($p = 10^{-4}$) because of the significant difference between activations during the LISTSENT-WORD task ($p = 10^{-3}$). Note that there was no significant difference between the asymmetries of LANG_CORE and LANG_VISU during the $LIST_{SENT\text{-}WORD}$ task ($p = 7.10^{-2}$).

LANG_EXE was the least activated network for the 3 tasks (all $p < 10^{-3}$).

Note that there were no significant differences in leftward asymmetry between the 3 tasks in LANG_EXE, LANG_DMN and LANG_VISU except between the $LIST_{SENT\text{-}WORD}$ and $READ_{SENT\text{-}WORD}$ tasks, where LANG_VISU had a larger asymmetry than LANG_EXE (each $p < 1.10^{-2}$).

***Assessing the reliability of the 4 networks identified in the 137 participants***

The AU p-values provided by the multiscale bootstrap resampling method showed that the 4 networks were reliable at levels of 91% for LANG_DMN, 89% for LANG_VISU, 87% for LANG_EXE and 86% for LANG_CORE.

***Robustness of the identified networks with respect to the clustering method***

The LANG_CORE network was identified by all 4 clustering methods, including at least 12 of the 16 hROIs initially

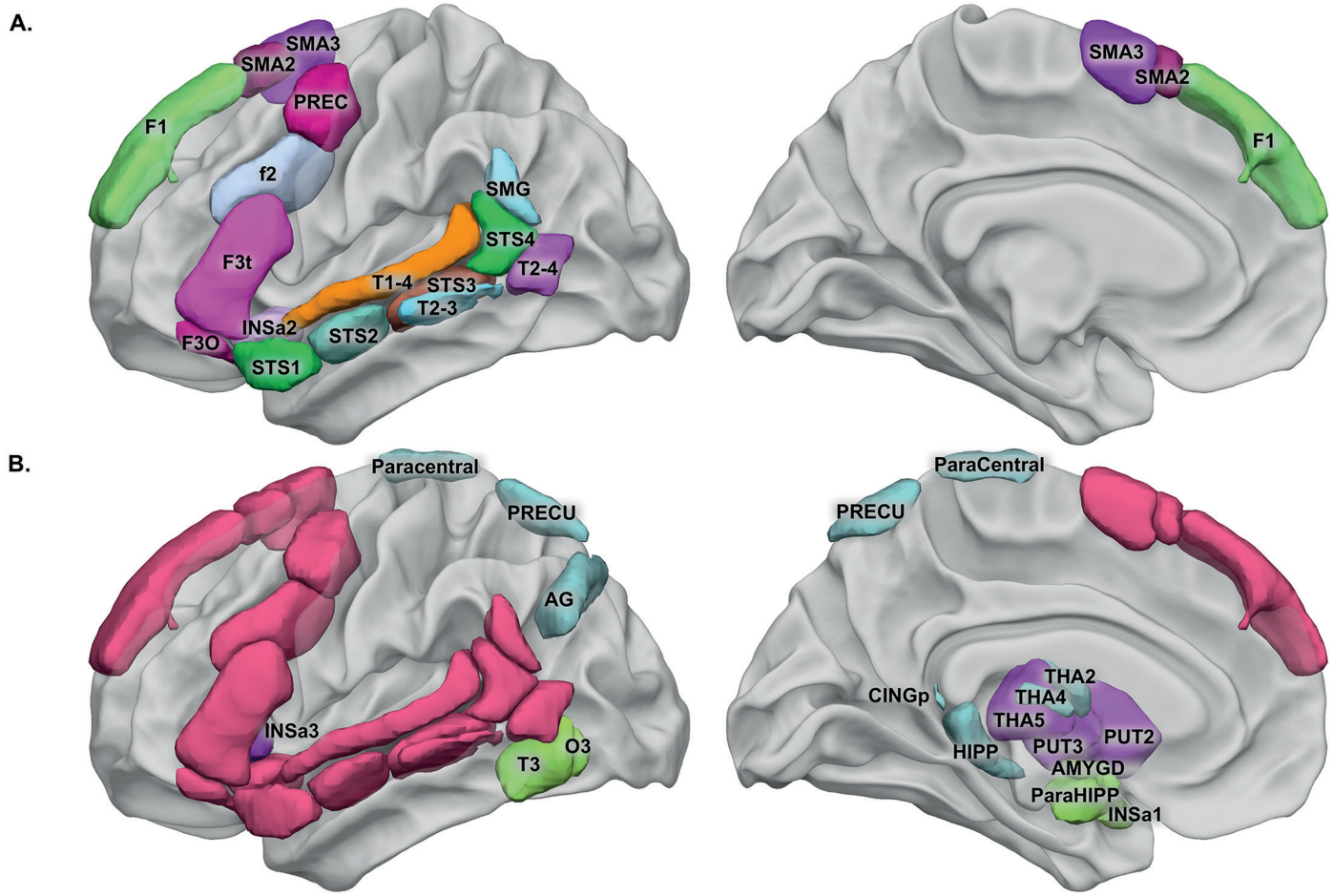


**Fig. 3** Lateral and medial views of the 4 identified networks. **a** Projection on the lateral surface of the left hemisphere of the MNI template with Surf Ice (https://www.nitrc.org/projects/surfice) of the 16 hROIs composing the LANG_CORE network. **b** Projection of the hROIs composing the 4 networks: LANG_CORE: pink, LANG_EXE: purple, LANG_DMN: light blue and LANG_VISU: green. Abbreviations for the hROIs of the AICHA atlas can be found in Table 2.

found with the aHCA method using the Ward's distance (see supplementary material Table 1). The aHCA method using the average distance method led to an adjusted Rand index of 1, indicating a clustering similar to that achieved using aHCA method with the Wards distance. Comparing the Gaussian Mixture Model and aHCA methods led to an adjusted Rand index of 0.83, indicating two highly similar partitions. Comparing the aHCA and k-Means methods led to the lowest adjusted Rand index of 0.66 (supplementary material Table 1).

### *Temporal correlation across networks and significance*

The chord diagram shown in Figure 4 describes the average correlations between each pair of hROIs in the 4 networks. Strong and highly significant correlations (Table 4) were found between LANG_CORE and LANG_EXE, which appeared to be the strongest positive correlation, between LANG_EXE and LANG_VISU, between LANG_DMN and LANG_EXE, and finally, between LANG_CORE and LANG_DMN, which appeared to be the strongest negative correlation.

By contrast, weak and non-significant correlations were observed between LANG_VISU and LANG_CORE and between LANG_VISU and LANG_DMN.

## Part 3. Graphical analysis of the lang_core network

We applied graphical analysis pairwise correlations, including only positive correlations since the inclusion of negative correlations in graphical analysis remains controversial (Rubinov & Sporns, 2010). Note that the graphical analysis of intra-network communication was completed for only LANG_CORE, as the other 3 networks had too few nodes.

## STATISTICAL ANALYSIS

### *Identification of hubs using graph analysis metrics of the networks*

#### *Measurements of weighted centrality*

We measured the degree centrality (DC) of the LANG_CORE network, corresponding to the sum of the strength of the positive correlation of each node (hROI). DC can thus be interpreted as the amount of information that a given hROI receives from the hROIs to which it is directly connected; i.e., the DC measures the importance of a given hROI within its network according to the number and strength of interactions it undergoes with the other

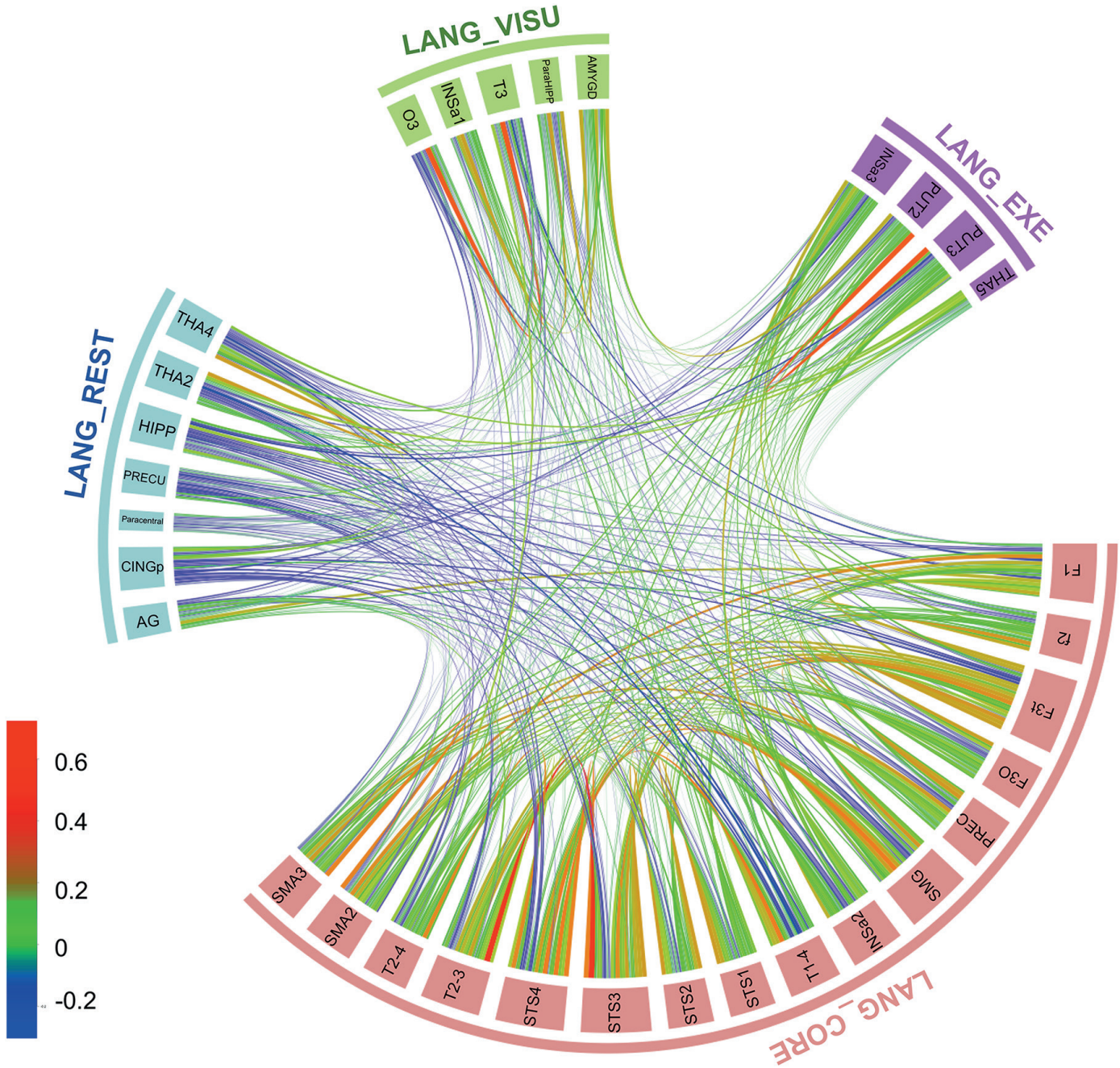


**Fig. 4** Chord diagram of the temporal correlation across each hROI composing the 4 networks averaged in the whole group. Abbreviations for hROIs of the AICHA atlas can be found in Table 2 (colour scale goes from red for positive correlation to blue for negative correlations, and the line width indicates the strength of the correlation).

| | Volume ($mm^3$) | Left | | | Leftward asymmetry | | |
|---|---|---|---|---|---|---|---|
| | | **$PROD_{SENT-WORD}$** | **$LIST_{SENT-WORD}$** | **$READ_{SENT-WORD}$** | **$PROD_{SENT-WORD}$** | **$LIST_{SENT-WORD}$** | **$READ_{SENT-WORD}$** |
| LANG_CORE | 75560 | 0.70 ± 0.30 | 0.43 ± 0.20 | 0.55 ± 0.25 | 0.39 ± 0.21 | 0.25 ± 0.14 | 0.29 ± 0.18 |
| LANG_EXE | 19544 | 0.33 ± 0.27 | 0.11 ± 0.17 | 0.10 ± 0.19 | 0.14 ± 0.13 | 0.05 ± 0.09 | 0.05 ± 0.11 |
| LANG_DMN | 14152 | 0.45 ± 0.34 | 0.28 ± 0.24 | 0.22 ± 0.25 | 0.18 ± 0.16 | 0.13 ± 0.16 | 0.10 ± 0.17 |
| LANG_VISU | 9952 | 0.45 ± 0.34 | 0.40 ± 0.25 | 0.32 ± 0.28 | 0.13 ± 0.19 | 0.168 ± 0.15 | 0.18 ± 0.18 |

**Table 3** Mean volumetric activation (and standard deviation) of the 4 language networks in each sentence minus word-list contrast for production (PRODSENT-WORD), listening (LISTSENT-WORD) and reading (READSENT-WORD) tasks in 137 healthy right-handers. The mean volumetric activation for a network was calculated from the sum of the activations of the ROIs comprising the network weighted by their individual volumes and then divided by the volume of the cluster.

hROIs.

The betweenness centrality (BC) was also measured for LANG_CORE as defined by Opsahl et al. (Opsahl, Agneessens, & Skvoretz, 2010). The BC of an hROI can be interpreted as the participation rate of that hROI in the set of shortest paths

| | LANG_CORE | LANG_DMN | LANG_VISU |
|---|---|---|---|
| **LANG_DMN** | -0.19* (81.0%, $p < 10^{-4}$) | - | - |
| **LANG_VISU** | -0.05 (58.39%, $p = 5.10^{-2}$) | 0.02 (55.47%, $p = 2.10^{-1}$) | - |
| **LANG_EXE** | 0.30* (93.3%, $p < 10^{4}$) | -0.07* (63.5%, $p < 10^{-3}$) | 0.13* (77.3%, $p < 10^{-4}$) |

**Table 4** Temporal correlations across networks and their significance. This table provides the correlations among the 4 networks and their significance as determined using a sign test. For each individual, the correlation between networks (LANG_CORE, LANG_DMN, LANG_VISU or LANG _EXE) was computed from the BOLD temporal signal averaged over all voxels composing each network. After z-transformation, these correlations were averaged across individuals. The table reports these mean correlation values after inverse z-transformation. The table also gives the fractions of positive correlation values (in parentheses) across the samples and their significance using a non-parametric sign test (with Bonferroni correction for the 6 possible correlations between the 4 networks).

between any pair of nodes within the network; i.e., BC measures the dependence of the network on a specific hROI for its communication.

*Hub definition and clustering*

To discriminate hubs among LANG_CORE, we applied a combination of Sporns (Sporns et al., 2007) and van den Heuvel (van den Heuvel, Mandl, Stam, Kahn, & Hulshoff Pol, 2010) definitions. We considered that an hROI had the properties of a hub when its DC and BC values were larger than the means plus one standard deviation of the DC and BC values of the hROI set in the network.

To assess whether the hubs identified in LANG_CORE participated in communication with the other 3 networks or whether its communication was only intra-LANG_CORE, we calculated the participation index (pIndex) criteria as defined by Guimera (Guimera & Amaral, 2005). hROIs having the 15% highest pIndex values were considered connector hubs (i.e., between networks) (van den Heuvel & Sporns, 2011), while the other hROIs corresponded to provincial hubs, i.e., an hROI communicating with only its own sub-network.

***Investigation of the relationship between intrinsic connectivity and activation measured during the language tasks***

*Relationships between DC and BOLD variation at the hROI level*

We investigated whether an hROI exhibiting high intrinsic connectivity with other areas of the LANG_CORE is more activated during language tasks. For this, we performed ANOVA with repeated measures with a TASK main effect, a DC main effect and a DC by TASK interaction. Linear regressions were computed between the DC and activation for each hROI and each task to calculate the corresponding correlation (R-values) and p-values. The p-values indicated whether an hROI was significant for the simple linear model investigated.

To test the specificity of this relationship, we completed similar ANOVAs with DC measurements obtained for the 184 hROIs of the AICHA atlas covering the entire left hemisphere. Therefore, the DC values were computed considering the connections of hROIs belonging to LANG_CORE with all other hROIs of the left hemisphere. This analysis made it possible to more deeply characterize whether the relationship between the DC and activation during the language tasks was specific to the essential language network intrinsic connectivity or whether this relationship was held at the hemispheric level.

Relationships between the DC measured in the LANG_CORE network and BOLD variation upon pooling all hROIs and participants.

To test whether the relationship previously identified between DC and BOLD signal variation for each hROI of LANG_CORE was a general property that could be extrapolated to any hROI of any participant, we applied the method proposed by Buckner for evaluating the relationship between DC and beta-amyloid accumulation in Alzheimer's disease (Buckner et al., 2009). Correlation coefficients obtained for the 3 tasks between DC values and BOLD variations were compared using the R package "cocor" function (Diedenhofen & Musch, 2015), to determine whether there was any difference across language tasks.

## Results

***Graph analysis of LANG_CORE***

*Sample distributions of DC and BC values*

DC variation across the hROIs spanned from 2.91 to 5.73 (Table 5), and the DC standard deviation was very consistent across hROIs ranging from 1.10 to 1.72.

By contrast, BC variation across the hROIs

spanned from 0.58 to 15.67 (Table 5). Notably, only 3 hROIs had low numbers of BC null values across the sample of 137 participants: F3t, STS3 and STS4 (1, 6 and 5% null values, respectively, Table 5).

*Hub identification and characterization*

3 hROIs corresponded to the hub definition, i.e., BC and DC values above the chosen significance thresholds (mean + SD) of 8.72 and 4.98, respectively (Table 5). The first hROI (F3t) was located in the frontal lobe, and the other two were located in the posterior third of the STS (STS3 and STS4). The BC values of these 3 hubs were over 11, and their DC values were over 5, with F3t having the strongest values (Figure 5). Note that no other hROI exhibited a supra-threshold value for one of the centrality indices.

Concerning the pIndex, hubs were defined as the top 15% of the highest index (pIndex ranging from 0.464 to 0.986). Five hROIs were thus defined as connector hubs: STS3 (pIndex = 0.986), T2-3 (pIndex = 0.984), F3t (pIndex = 0.980), SMG (pIndex = 0.978), and STS4 (pIndex = 0.977).

Note that the centrality hubs F3t, STS3 and STS4 were also connector hubs, meaning that they are important for both communication among the 4 different networks and for communication within the LANG_CORE network. T2-3 and SMG were identified as only connector hubs; however, both hROIs were characterized by high DC and BC values, although they did not meet the criteria to be labelled centrality hubs (Figure 5).

***Relationship between the DC at rest and activations during the language tasks in the LANG_CORE network***

*Relationship at the individual hROI level*

Using DC values computed from only LANG_CORE hROIs, we observed significant positive correlations between activations during the 3 language tasks, and these DC values were observed in 13 hROIs among the 16 constituting LANG_CORE (Table 6). Among these hROIs, DC values were positively correlated with activations during

| | AICHA hROI | Betweenness Centrality | | | Degree Centrality | | | | |
|---|---|---|---|---|---|---|---|---|---|
| | | Mean | SD | % null values | Mean | SD | Skewness | Kurtosis | p norm |
| *Frontal & insula* | PREC | 4.07 | 5.49 | 34 | 4.08 | 1.32 | -0.21 | 0.31 | 0.21 |
| | F1 | 2.17 | 3.33 | 48 | 4.08 | 1.27 | -0.05 | 0.09 | 0.94 |
| | f2 | 1.09 | 3.08 | 76 | 2.91 | 1.42 | 0.18 | 0.56 | 0.009 |
| | F3t | 15.67 | 8.76 | 1 | 5.73 | 1.12 | 0.00 | 0.27 | 0.72 |
| | F3O | 1.39 | 3.12 | 72 | 3.54 | 1.46 | -0.62 | 0.29 | 0.03 |
| | INSa2 | 0.58 | 1.81 | 81 | 3.20 | 1.31 | -0.18 | 0.25 | 0.35 |
| *Temporal & parietal* | T1-4 | 1.28 | 2.86 | 68 | 3.27 | 1.42 | -0.69 | 0.42 | 0.001 |
| | T2-3 | 3.24 | 5.00 | 41 | 4.81 | 1.24 | 0.07 | 0.03 | 0.82 |
| | T2-4 | 0.75 | 1.98 | 80 | 3.03 | 1.72 | -0.51 | 0.45 | 0.003 |
| | STS1 | 1.72 | 3.04 | 55 | 3.71 | 1.31 | 0.20 | 0.15 | 0.73 |
| | STS2 | 1.40 | 2.70 | 61 | 3.68 | 1.38 | -0.23 | 0.50 | 0.004 |
| | STS3 | 11.24 | 8.37 | 6 | 5.73 | 1.23 | -0.33 | -0.14 | 0.70 |
| | STS4 | 11.91 | 7.78 | 5 | 5.12 | 1.31 | 0.08 | 0.14 | 0.45 |
| | SMG | 5.35 | 6.18 | 29 | 4.89 | 1.32 | -0.29 | -0.07 | 0.91 |
| *Internal surface* | SMA2 | 1.62 | 2.82 | 43 | 3.88 | 1.10 | -0.20 | 0.08 | 0.72 |
| | SMA3 | 1.27 | 2.80 | 61 | 3.61 | 1.20 | -0.49 | 0.36 | 0.03 |

**Table 5** Betweenness and degree centrality of LANG_CORE hROIs. The means and standard deviations (SD) of the betweenness centrality (BC) and degree centrality (DC) were computed by averaging the BC and DC values of each participant for each LANG_CORE hROI. For BC, the percentage of null values is based on the number of BC values at zero among the 137 subjects for one hROI. For DC, the skewness, kurtosis and Shapiro-Wilk normality test (p norm) correspond to information regarding the normality of the DC distribution for each hROI. A value above 0.05 for the Shapiro-Wilk normality test indicates that the DC was normally distributed. hROIs in bold are those we found to be hubs.

the language tasks. Moreover, in 10 of these 13 hROIs, there was no DC by Task interaction, meaning that the correlation between the DC and activation did not differ between the tasks. In the f2, F3t, T1-4 and SMG hROIs, a significant DC by Task interaction was observed. In f2, the interaction was due to non-significant correlation for the production task contrast, while the correlation was strong and significant for the reading and listening task contrasts. In F3t, the interaction was due to stronger correlation during production, while the interactions in SMG and T1-4 were due to lower correlations during listening (Table 6).

The results obtained using DC values computed from the entire set of 184 left hemisphere hROIs were strikingly different. There was a significant main effect of the DC in only 4 hROIs (F1, F3t, T2-3 and STS3, see supplementary material), meaning that except for these four regions, the strength of the correlation when measured across the entire hemisphere did not explain the activation amplitude in LANG_CORE hROIs. In addition, in these 4 hROIs, the correlation between the DC and the activation amplitude was weak, ranging from 0.035 to 0.054.

*Relationship at the global level using all participants and hROIs*

There was a significant correlation between the DC values and BOLD variations measured in each of the 3 tasks when considering the 16 LANG_CORE hROIs and the 137 participants in a single analysis (Figure 6) for each task. The coefficient correlation values were 0.138, 0.173 and 0.227 for sentence production, sentence listening and sentence reading, respectively. The correlation for reading was significantly larger than that for both listening ($p = 0.001$) and production ($p = 0.002$), and the latter two were not significantly different ($p = 0.18$).

## Summary of results

Conjunction analysis of left activated and leftward asymmetrical hROIs in 144 right-handed participants performing three language tasks ($PROD_{SENT\text{-}WORD}$, $READ_{SENT\text{-}WORD}$ and $LIST_{SENT\text{-}WORD}$) uncovered a set of 32 supramodal regions involved in lexico-syntactic processing. The hierarchical bottom-up clustering of the intrinsic connectivity between these 32 hROIs led to the identification of 4 networks: a network of essential language areas (LANG_CORE), a network of executive areas recruited by the language tasks (LANG_EXE), a network of visual language areas at the interface between visual and syntactic processing (LANG_VISU), and a network of DMN areas (LANG_DMN). Intrinsic connectivity analysis showed that while LANG_CORE was positively correlated with LANG_EXE, it was negatively correlated with LANG_DMN. Graphical metrics obtained for the LANG_CORE network revealed that F3t, STS3, and STS4 were hubs of both degree and betweenness connectivity as well as of participation, meaning that these are key areas for both intra-network communication and inter-network communication between LANG_CORE and the other 3 networks. Importantly, a positive correlation across individuals was observed between the DC measured at rest in LANG_CORE and the strength of activation in most LANG_CORE regions, meaning that participants with

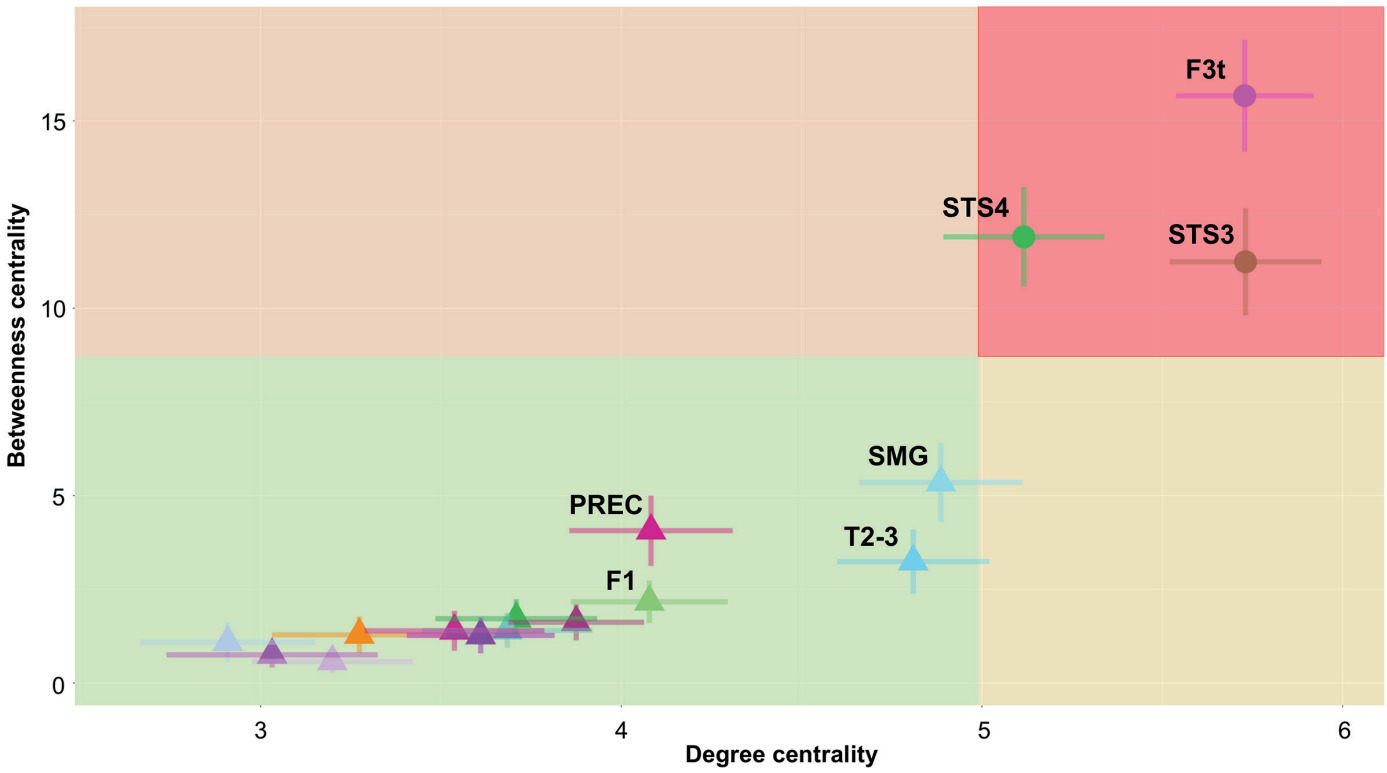


**Fig. 5** Plot of degree centrality (DC) versus betweenness centrality (BC) in LANG_CORE. The mean plus standard deviation values of DC and BC define the quadrants. hROIs located in the superior right quadrant are hubs. Abbreviations for the hROIs of the AICHA atlas can be found in Table 2.

| | AICHA hROI | ANOVA | | $PROD_{SENT-WORD}$ | | $LIST_{SENT-WORD}$ | | $READ_{SENT-WORD}$ | |
|---|---|---|---|---|---|---|---|---|---|
| | | DC | DC*Task | R | p | R | p | R | p |
| Frontal & insula | PREC* | 0.018 | 0.46 | 0.2 | 0.027 | 0.165 | 0.053 | 0.1 | 0.25 |
| | F1 | 0.144 | 0.552 | 0.132 | 0.12 | 0.112 | 0.19 | 0.028 | 0.75 |
| | f2* | 0.019 | 0.0003 | -0.085 | 0.32 | 0.256 | 0.0025 | 0.304 | 0.0003 |
| | F3t* | <0.0001 | 0.049 | 0.342 | <.0001 | 0.224 | 0.0083 | 0.244 | 0.004 |
| | F3O* | 0.0004 | 0.48 | 0.229 | 0.007 | 0.233 | 0.006 | 0.224 | 0.008 |
| | INSa2* | 0.0003 | 0.08 | 0.27 | 0.0014 | 0.145 | 0.09 | 0.246 | 0.004 |
| Temporal & parietal | T1-4* | 0.0014 | 0.036 | 0.225 | 0.008 | 0.089 | 0.3021 | 0.282 | 0.0008 |
| | T2-3* | 0.002 | 0.38 | 0.257 | 0.002 | 0.208 | 0.015 | 0.145 | 0.09 |
| | T2-4* | 0.0014 | 0.23 | 0.183 | 0.033 | 0.245 | 0.0039 | 0.277 | 0.001 |
| | STS1* | 0.0002 | 0.23 | 0.258 | 0.0024 | 0.218 | 0.01 | 0.28 | 0.0009 |
| | STS2 | 0.39 | 0.78 | 0.098 | 0.25 | 0.046 | 0.6 | 0.045 | 0.6 |
| | STS3* | 0.011 | 0.39 | 0.216 | 0.011 | 0.216 | 0.011 | 0.119 | 0.16 |
| | STS4* | 0.008 | 0.28 | 0.285 | 0.0007 | 0.202 | 0.018 | 0.255 | 0.0026 |
| | SMG* | <0.0001 | 0.015 | 0.314 | 0.0002 | 0.215 | 0.012 | 0.311 | 0.0002 |
| Internal surface | SMA2 | 0.52 | 0.16 | 0.123 | 0.15 | -0.006 | 0.95 | -0.05 | 0.56 |
| | SMA3* | 0.002 | 0.09 | 0.25 | 0.003 | 0.127 | 0.14 | 0.169 | 0.05 |

**Table 6** Correlation analysis between the degree centrality measured in the LANG_CORE network and the mean activation in each of the 3 language tasks. Correlations (R) were calculated within each hROI of the left hemisphere constituting the LANG_CORE network, and the DC values were calculated in the LANG_CORE network. hROIs with a star (*) are those with significant correlations between activation and DC values ($p < 0.05$).

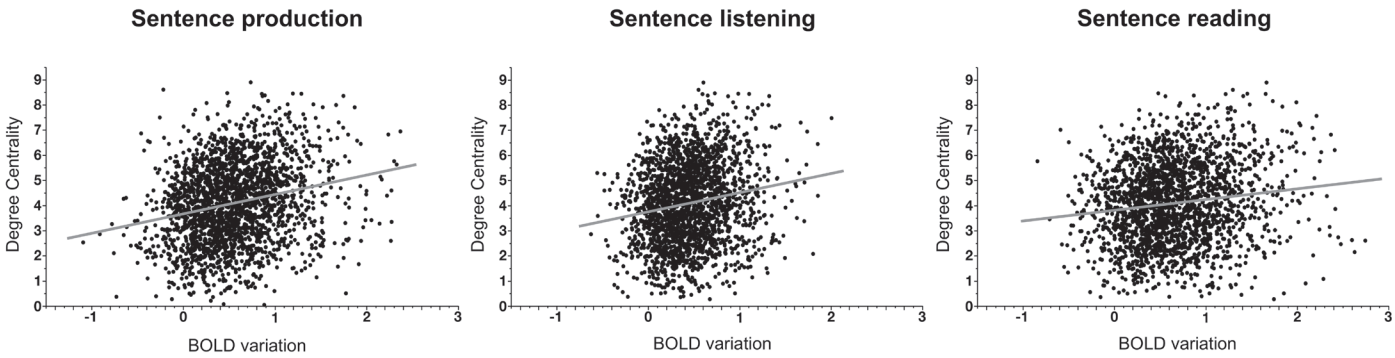


**Fig. 6** Correlation between DC values and activations in LANG_CORE across participants and across the 16 hROIs during each of the 3 language tasks. Plots of DC values and BOLD variations of the sentence minus word contrasts calculated for sentence production (left), sentence listening (middle), sentence reading (right) and degree centrality. The positive correlation coefficients (N = 137*16 = 2192) are 0.138 for sentence production, 0.173 for sentence listening, and 0.227 for sentence reading.

larger DC values in a given region had higher activations than participants with lower DC values. Moreover, such a positive correlation between the DC and activation was still significant when all regions of all participants in the 3 tasks were pooled, meaning that this was true regardless of the cortical area considered.

## Discussion

### Methodological issues

In this study, we selected right-handers from the BIL&GIN database because we previously demonstrated that these participants have a left hemisphere dominance for language at both the group level (Tzourio-Mazoyer, Joliot, Marie, & Mazoyer, 2016) and the individual level (Zago et al., 2017), with only 5 (3%) of the 144 participants having a co-dominant right hemisphere. This sample group is optimal for selecting areas specific for sentence processing

based on a conjunction of activations and leftward asymmetries. In addition, the inclusion of a fairly considerable number of participants (N = 144) provided us a high sensitivity for detecting supramodal sentence areas while minimizing the risk of overlooking some.

However, we must underline that the present atlas is not all-inclusive. First, we selected map regions involved in only high-order language processing and lexico-syntactic processing. Using the list of familiar words as the reference condition, we removed the dorsal route of language, including the phonological loop, responsible for articulation and sound to articulation mapping (Rauschecker & Scott, 2009; Saur et al., 2008). In addition, the regions selected herein focused on the left hemisphere and did not account for right hemisphere-specialized aspects of sentence processing, such as emotional prosody (Beaucousin et al., 2007; Hurschler, Liem, Jäncke, & Meyer, 2013) and context processing (Ferstl, Rinck, & Cramon, 2005; Grindrod & Baum, 2003).

Second, the presence of susceptibility artefacts combined with averaging the large number of participants led to incomplete mapping of the inferior part of the temporal lobe, prohibiting us from documenting some areas, such as the basal language area in the anterior part of the fusiform gyrus. This essential language area, first identified using deep electrical recordings (Nobre, Allison, & McCarthy, 1994), has been shown with positron emission tomography (PET) to be activated during both the production and auditory comprehension of language (Papathanassiou et al., 2000).

Third, small size regions may also be lacking in this atlas since we provided data at the hROI scale rather than at the voxel scale.

Concerning the clustering methods, a perfect match was observed between the Ward's and average clustering methods (see supplementary material Table 1), and a good score was obtained with the Gaussian Mixture Model for global clustering at the 32 hROI levels. The weakest score was that of the k-Means method, which gathered only 75% of the LANG_CORE hROIs. Such a difference in clustering observed with k-Means compared to that in the other 3 methods is consistent with the fact that, as reported by Thirion et al., k-Means forms clusters spatially close and connected but with poor reproducibility using the sample studied. By contrast, hierarchical clustering using Ward's method, which we selected to segregate the networks, was reported to create connected clusters that are highly reproducible using the samples studied (Thirion, Varoquaux, & Dohmatob…, 2014). A comparison of the 3 consistent clustering methods (excluding K-Means) showed a low impact of the method used to identify the different networks among the 32 regions that were co-activated and co-leftward asymmetrical across tasks. Only one hROI of LANG_CORE (T2-4) was excluded by 2 clustering methods other than Ward's, while all 15 other hROIs were classified together by at least 3 different clustering methods.

**A large set of supramodal language areas are involved in sentence processing tasks**

We carefully designed each of the language tasks such that joint analyses were possible; the design was identical in the 3 tasks, and we chose to make them close enough to allow comparisons and conjunctions in terms of the number of words or the complexity of sentences. As mentioned above, the use of a high-level verbal reference task for controlling the involvement of primary areas (auditory, visual and motor) and removing phonological and automatic word processing kept the lexico-syntactic aspects common to all three tasks.

The first set of 32 hROIs provides left hemispheric regions that are dedicated to the monitoring and completion of tasks based on sentence processing. Although not all regions can be considered essential language areas, all were determined to be modulated by the verbal material with which they are associated (left activation and leftward asymmetry) and are thus part of an extended language network functioning during language tasks.

Within this large set of 32 hROIs, unsupervised hierarchical clustering based on the resting-state connectivity between hROIs was successful at segregating different networks, including networks hosting core language, visual and executive areas as well as parts of the DMN. Within the systems to which they belonged, these networks hosted areas dedicated to the interaction/interface with language systems. For example, the current analysis extracted among the visual areas involved by the picture processing, those areas specifically dealing with picture-sentence meaning integration.

**Language comprehension essential network (LANG_CORE)**

Clustering the resting-state correlation between these 32 hROIs allowed for discriminating LANG_CORE, a network of 16 strongly and positively correlated hROIs, mainly including frontal and temporal hROIs located on the lateral surface of the left hemisphere. In particular, LANG_CORE included areas of the antero-posterior language networks, named in reference to the Broca-Wernicke model in aphasia literature and reported with consistency in meta-analyses of healthy individuals mapped during language tasks (Price, 2010; Price, 2012; Vigneau et al., 2006). Note that LANG_CORE was the largest network in terms of volume (in mm3), as it included half of the hROIs (16/32), all which were strongly activated and leftward asymmetrical. In the frontal lobe, LANG_CORE included the inferior frontal gyrus (F3t), corresponding to Broca's area according to most authors, whose lesion is responsible for conversational deficits, as is also the case for the anterior insula (INSANT2) (Borovsky, Saygin, Bates, & Dronkers, 2007). The posterior part of the inferior frontal sulcus (f2) and the junction between the precentral and middle frontal gyrus (PREC), also part of LANG_CORE, have been underlined as areas involved in

lexico-syntactic processing (Vigneau et al., 2006). Price also targeted PREC and f2 as being involved in word selection and hierarchical sequencing (Price, 2010). Another indication of the important role of this area can be found in the fact that PREC and f2 (together with F3t) show atrophy in non-fluent progressive primary aphasia (PPA) (Mesulam et al., 2014; Wilson et al., 2010).

In the medial part of the frontal lobe, LANG_CORE included both preSMA and the superior frontal gyrus (here SMA2, SMA3 and F1), which have been reported in tasks involving sentences dealing with characters (Hervé, Razafimandimby, Vigneau, Mazoyer, & Tzourio-Mazoyer, 2012), like in the present paradigm. Their activation has been attributed to processing the social aspects of verbal material (Ferstl & von Cramon, 2002). As it will be later developed these medial frontal areas are strongly connected with the posterior part of the middle temporal gyrus (Turken & Dronkers, 2011). Notably, these medial frontal areas are also the sites of atrophy in PPA (Tetzloff et al., 2018; Wilson et al., 2010).

In the temporal lobe, LANG_CORE included the STS together with the posterior part of the middle and superior temporal gyri, extending to the angular and supramarginal gyri. This is consistent with the proposal by Price that these areas are involved in amodal semantic combinations, a process common to the 3 sentence tasks (Price, 2010). Moreover, these posterior temporal areas have been documented to be essential language areas since the lesion of each results in specific deficits in sentence comprehension (Dronkers et al., 2004). Furthermore, the posterior parts of the middle temporal gyrus and STS show specific atrophy in logopenic PPA (Wilson et al., 2010).

The similitude between the areas composing the LANG_CORE network and the regions showing atrophy in all types of PPA (Mesulam et al., 2014) is striking and a key element to concluding that LANG_CORE contains essential language areas, although the inferior temporal and fusiform gyri are lacking for the methodological reasons mentioned above.

LANG_CORE frontal and temporal areas were shown to constitute a network of highly connected areas at rest by Turken (Turken & Dronkers, 2011). The similarity between the regions found by these authors when seeding the posterior part of the middle temporal gyrus and the areas constituting LANG_CORE is clear.

The putamen and thalamus are part of LANG_CORE, and both are responsible for aphasia when lesioned. Lesions of the left putamen cause non-fluent aphasia, and when associated with frontal lesions, cause mutism, while left thalamic lesions are associated with word-finding and picture-naming difficulties (Kreisler et al., 2000).

## Hubs of LANG_CORE

The computation of betweenness and degree centralities allowed us to identify 3 hubs within LANG_CORE: one in the inferior frontal gyrus (F3t) and two others (STS3 and STS4) along the posterior part of the temporal cortex. These high centrality measurements demonstrate that these hROIs are central in communications with other parts of LANG_CORE, and their participation indices further indicate their essentiality for communication with the other networks identified in language. Such properties are consistent with the definition of epicentres proposed by Mesulam (Mesulam, 1998), and these regions can be considered essential for sentence/test comprehension independent of the modality. According to Mesulam, the network epicentre specializes in a specific behavioural component, which is language in this study, and the destruction of transmodal epicentres causes global impairments. Actually, these hROIs overlap the middle temporal gyrus targeted in the aphasics investigation by Dronkers (Dronkers et al., 2004) and Turken (Turken & Dronkers, 2011) as well as the regions showing the highest atrophy in all types of PPA (Mesulam et al., 2014; Wilson et al., 2010), confirming that they do correspond to epicentres. In addition, these hubs are distributed in the anterior and posterior cortices, constituting an antero-posterior loop across areas belonging to the same hierarchical level in terms of cortical organization, consistent with Fuster's model for cognition (Fuster & Bressler, 2012). Such a framework is also thought to correspond to the Broca-Wernicke language model, with F3t serving as Broca's area and STS3 and STS4 serving as regions involved in the supramodal integration of meaning, consistent with the location of posterior areas leading to comprehension deficits (Pillay et al., 2017). These posterior STS areas are also considered by Binder as areas supporting meaning integration during sentence comprehension (Binder, 2017). Considering that a left deficit in this area leads to deficits in language comprehension, we propose to label it Wernicke's area, although as reviewed by Binder, such a definition is different from the location currently proposed for Wernicke's area in the superior temporal gyrus. In the present work, closely adhering to an anatomo-functional definition in reference to deficits in comprehension associated with Wernicke's aphasia (Binder, 2015; Binder, 2017; Dronkers et al., 2004), we propose that F3t, STS3 and STS4, regions strongly activated and asymmetrical during sentence processing in different modalities and hubs of the LANG_CORE network, are the epicentres of sentence comprehension.

## Other networks contributing to the language tasks

Because each event of the sentence tasks included task monitoring, such as shifting between the word list and sentence tasks when a picture was presented or providing a motor response at the end of sentence processing, the involvement of executive areas was expected. Conjunction analyses revealed that the anterior insula was at play in the 3 tasks, previously shown by Zago as part of supramodal executive areas (Zago et al., 2008). This region constituted a network with putamen hROIs, and we named it LANG_EXE because as the anterior insula, putamen is a key neural support area of executive functions and task monitoring

(Monchi, Petrides, Strafella, Worsley, & Doyon, 2006; Sefcsik et al., 2009). Moreover, a recent meta-analysis involving connectivity modelling showed that the left and right putamen areas are different in terms of their respective co-activations, which are specifically co-involved in language areas (Viñas-Guasch & Wu, 2017). The thalamic hROI that was part of the LANG_EXE network comprised large, overlapping lateral and ventro-lateral nuclei of the thalamus, which are involved in linguistic functions (Klostermann, Krugel, & Ehlen, 2013). This network showed higher activity and asymmetry during language production, which was the task most reliant on executive functions and was considered the most difficult by the participants.

The LANG_EXE network had low involvement during the language tasks, as determined by its low mean activation and asymmetry. However, this network was synchronized with LANG_CORE, and the positive correlation between these two networks was strong, consistent with the role of the thalamus and anterior insula in language functions. The anterior insula is actually involved in both language production (Baldo et al., 2011; Dronkers & Ogar, 2004; Dronkers, 1996) and executive functions (Zago & Tzourio-Mazoyer, 2002).

The two other networks showed negative correlations with LANG_CORE. One was LANG_DMN, which included THA2 (located in the anterior pole of the thalamus) and THA4 (located medially), both of which are known to be strongly connected with medial cortical areas and the Papez circuit (Jankowski et al., 2013). This is consistent with their clustering with the hippocampus, posterior cingulate, precuneus, and paracentral lobule. The hippocampus, posterior cingulate, precuneus, and angular gyrus are part of the DMN, which has been shown to be involved in both episodic thinking and self-processing. Task-induced activation studies have demonstrated that these areas are also part of mind-reading areas (Spreng, Mar, & Kim, 2009). In the present paradigm, these areas were at play as the participants dealt with drawings and sentences depicting social interactions. Activated and leftward lateralized during language tasks, this set of areas belonging to the DMN likely interacts with LANG_CORE during language tasks related to sentence content dealing with social interactions (Hervé et al., 2012). The angular gyrus was segregated with this LANG_DMN network. This area is actually considered part of the DMN (Raichle, 2015) but is also involved in lexico-semantic processing, as identified by language task-induced activation studies (Price, 2010; Vigneau et al., 2006). A careful examination of the correlation matrix shows that the angular hROI was positively correlated with 9 of the 16 language areas constituting LANG_CORE, although its correlation profile was closer to that of the DMN areas. This is important since the angular gyrus is involved in conceptual knowledge, as its lesions lead to the inability to associate a sound or image related to the same concept (Saygin, Wilson, Dronkers, & Bates, 2004). Inactivation of this area in the left hemisphere was recently shown to induce a deficit in semantic integration (Price, Peelle, Bonner, Grossman, & Hamilton, 2016). Combining resting-state and co-activation data measured from a meta-analysis to functionally parcel the inferior parietal lobule, Wang et al. (Wang et al., 2017) confirmed this hypothesis. The angular hROI identified herein corresponds to Wang's C5 and C6 parcels, shown to be involved in both language and theory-of-mind tasks.

Finally, the fourth network included visual regions at the junction of the posterior part of the inferior temporal lobe and the occipital lobe. These areas are likely related to visual processing associated with the one-second drawing presentation (minus the scramble version of the word-list reference tasks) common to all tasks. Actually, in her meta-analysis, Price considered these areas direct visual combinations (Price, 2010), consistent with the design of the present paradigm wherein the participants dealt with images related to sentence content regardless of the sentence task modality and the fact that the mean value and asymmetry of this network did not vary with the language tasks. Interestingly, these visual regions were clustered with internal temporal regions surrounding the amygdala, suggesting that the later network is involved in the processing of visual and affective image content in relation to verbal content. Importantly, at rest, the correlation between the LANG_VISU and LANG_CORE networks was negative, with a trend towards significance, meaning that their intrinsic activities were asynchronous. The areas involved in visual and emotional processing that did not constitute a network at rest with language areas showed a strong leftward activation lateralization during the language tasks, suggesting that their involvement during sentence presentation in association with meaningful images is subject to top-down influences from language networks.

**The degree of centrality measured in lang_core explains the activation variability during the 3 language tasks**

To our knowledge, we are the first to report a positive correlation between the DC and task-induced activation values. All of the correlations between DC values and hROI activations were positive; the mechanism underlying this result may be that regions more highly connected within a network are more highly recruited during language tasks. It is also important to note that for 10 of the 13 hROIs, no significant effect of the nature of the task on the correlation strength was observed; the positive correlation did not differ regardless of whether the participants produced, read or listened to sentences compared to listing words. Such a relationship was also true when plotting all LANG_CORE regions of all subjects, as done by others in a different context (Buckner et al., 2009), meaning that this relationship between resting-state intrinsic connectivity and activation strength is true regardless of the participant and cortical area being considered. In Buckner's study, the authors hypothesized that beta amyloid accumulates in high DC regions because their high metabolism makes them more vulnerable to the disease, consistent

with the report that the DC calculated at the voxel level in the entire hemisphere is correlated with cerebral blood flow values (Liang, Zou, He, & Yang, 2013). The DC values in LANG_CORE may also indicate the metabolism of language areas in a given individual, which may be of interest in the evaluation of pathological states. Mesulam et al. reported the selective atrophy of right hemisphere areas in a PPA patient with right hemisphere dominance for language, an observation suggesting that language networks are specifically targeted by this illness (Mesulam, Weintraub, Parrish, & Gitelman, 2005). DC measurements in LAN_CORE may be a valuable index to evaluate inter-individual variations in language area activities in relation to anatomical and clinical patterns in such pathologies.

Previous investigations dealing with the relationships between tasks and the resting state have compared the functional connectivity during cognitive tasks with that measured during the resting state (Cole, Bassett, Power, Braver, & Petersen, 2014; Gerchen & Kirsch, 2017), as reviewed by Wig ((Wig, 2017)). Reports more closely related to the approach used herein have compared the resting-state connectivity and hemispheric activation asymmetries obtained during language production in healthy individuals (Joliot, Tzourio-Mazoyer, & Mazoyer, 2016) and schizophrenic patients (Doucet et al., 2015). Other investigations have found correlations between the task-induced and intrinsic connectivity asymmetries measured in selected sets of ROIs (Liu, Stufflebeam, Sepulcre, Hedden, & Buckner, 2009), such as the set of regions involved in a semantic decision task (Wang, Buckner, & Liu, 2014). The results across these studies consistently show that asymmetries of intrinsic connectivity partially explain the variability in activation asymmetries measured during language tasks. However, to our knowledge, there are no previous reports of a relationship between DC and activation strength, probably because such a relationship is lacking when comparing whole-brain intrinsic connectivity to variations in activity triggered by cognitive tasks that are underpinned by specific networks. In fact, in the present study, this relationship was observed when the DC computation considered only the 16 hROIs of the LANG_CORE network and disappeared when the DC computation included all of the left hemisphere hROIs. This is an important observation because it underlines the necessity of exploring the properties of intrinsic connectivity within specific networks rather than at the whole-brain level.

Considering that the rs-fMRI acquisition was completed on average 11 months before the language fMRI session herein, it was surprising that the rs-fMRI-derived DC values explained up to 12% of the variance in the language fMRI-derived activation amplitudes in 13 of the 16 LANG_CORE network regions. Thus, DC values at rest in regions constituting LANG_CORE can be considered proxies of their potential involvement during sentence processing. However, to generalize this observation, we need to both investigate how the LANG_CORE DC is modified in individuals atypical for language and confirm that such a relationship between the DC value during the resting state and activation strength also exists for networks supporting other cognitive domains, specifically the attentional system, in the same participant.

## Conclusion

Based on the fMRI analysis of 3 language tasks performed by 144 healthy adult right-handers combined with the analysis of intrinsic resting-state connectivity in 137 of the participants, we propose a FALCON atlas of high-order language processing areas. This atlas includes 32 regions decomposed into 4 networks, including one (LANG_CORE) specifically composed of essential areas for sentence reading, listening and production. This atlas also contains the features of these 4 networks, a graph analysis of the intrinsic connectivity of regions that compose LANG_CORE (their degree centrality values that correlate with their strength of activation during the language tasks) as well as the relationships across the different language networks at rest. Such a positive correlation between the DC at rest and the language task-induced activation amplitude in the left hemisphere language network opens the way for investigating participants with language pathologies or population neuroimaging studies searching for the genetic basis of language by analysing only resting-state acquisition. Finally, the methodology we applied, identifying regions from activation studies for selecting the networks at play, advanced the specificity of resting-state graphical analysis and shed light on the relationships between resting-state and task-related networks.

## References


Amunts, K., & Zilles, K. (2012). Architecture and organizational principles of Broca's region. Trends Cogn Sci, 16(8), 418-426.

Baldo, J. V., Wilkins, D. P., Ogar, J., Willock, S., & Dronkers, N. F. (2011). Role of the precentral gyrus of the insula in complex articulation. Cortex, 47(7), 800-807.

Beaucousin, V., Lacheret, A., Turbelin, M. R., Morel, M., Mazoyer, B., & Tzourio-Mazoyer, N. (2007). FMRI study of emotional speech comprehension. Cereb Cortex, 17(2), 339-352.

Binder, J. R. (2011). Functional MRI is a valid noninvasive alternative to Wada testing. Epilepsy Behav, 20(2), 214-222.

Binder, J. R. (2015). The Wernicke area Modern evidence and a reinterpretation. Neurology.

Binder, J. R. (2017). Current Controversies on Wernicke's Area and its Role in Language. Curr Neurol Neurosci Rep, 17(8), 58.

Borovsky, A., Saygin, A. P., Bates, E., & Dronkers, N. (2007). Lesion correlates of conversational speech production deficits. Neuropsychologia, 45(11), 2525-2533.

Buckner, R. L., Sepulcre, J., Talukdar, T., Krienen, F. M., Liu, H., Hedden, T., . . . Johnson, K. A. (2009). Cortical hubs revealed by intrinsic functional connectivity: mapping, assessment of stability, and relation to Alzheimer's disease. J Neurosci, 29(6), 1860-1873.

Charrad, M., Ghazzali, N., Boiteau, V., Niknafs, A., & Charrad, M. M. (2014). Package 'NbClust'. Journal of Statistical Software, 61, 1-36.

Clos, M., Amunts, K., Laird, A. R., Fox, P. T., & Eickhoff, S. B. (2013). Tackling the multifunctional nature of Broca's region meta-analytically: co-activation-based parcellation of area 44. Neuroimage, 83, 174-188.

Cole, M. W., Bassett, D. S., Power, J. D., Braver, T. S., & Petersen, S. E. (2014). Intrinsic and task-evoked network architectures of the human brain. Neuron, 83(1), 238-251.

Diedenhofen, B., & Musch, J. (2015). cocor: a comprehensive solution for the statistical comparison of correlations. PLoS One, 10(3), e0121945.

Dodoo-Schittko, F., Rosengarth, K., Doenitz, C., & Greenlee, M. W. (2012). Assessing language dominance with functional MRI: the role of control tasks and statistical analysis. Neuropsychologia, 50(11), 2684-2691.

Doucet, G. E., Pustina, D., Skidmore, C., Sharan, A., Sperling, M. R., & Tracy, J. I. (2015). Resting-state functional connectivity predicts the strength of hemispheric lateralization for language processing in temporal lobe epilepsy and normals. Hum Brain Mapp, 36(1), 288-303.

Dronkers, N., & Ogar, J. (2004). Brain areas involved in speech production. Brain, 127(Pt 7), 1461-1462.
Dronkers, N. F. (1996). A new brain region for coordinating speech articulation. Nature.

Dronkers, N. F., Wilkins, D. P., Van Valin, R. D., Redfern, B. B., & Jaeger, J. J. (2004). Lesion analysis of the brain areas involved in language comprehension. Cognition, 92(1-2), 145-177.

Duda, R. O., Hart, P. E., & Stork, D. G. (2012). Pattern classification.

Dym, R. J., Burns, J., Freeman, K., & Lipton, M. L. (2011). Is functional MR imaging assessment of hemispheric language dominance as good as the Wada test?: a meta-analysis. Radiology, 261(2), 446-455.

Efron, B., Halloran, E., & Holmes, S. (1996). Bootstrap confidence levels for phylogenetic trees. Proceedings of the National Academy of Sciences, 93(23), 13429-13429.

Ferstl, E. C., Neumann, J., Bogler, C., & von Cramon, D. Y. (2008). The extended language network: a meta-analysis of neuroimaging studies on text comprehension. Hum Brain Mapp, 29(5), 581-593.

Ferstl, E. C., Rinck, M., & Cramon, D. Y. V. (2005). Emotional and temporal aspects of situation model processing during text comprehension: An event-related fMRI study. Journal of cognitive Neuroscience, 17(5), 724-739.

Ferstl, E. C., & von Cramon, D. Y. (2002). What Does the Frontomedian Cortex Contribute to Language Processing: Coherence or Theory of Mind. NeuroImage, 17(3), 1599-1612.

Friederici, A. D., & Gierhan, S. M. (2013). The language network. Curr Opin Neurobiol, 23(2), 250-254.
Fuster, J. M., & Bressler, S. L. (2012). Cognit activation: a mechanism enabling temporal integration in working memory. Trends Cogn Sci, 16(4), 207-218.

Gerchen, M. F., & Kirsch, P. (2017). Combining task-related activation and connectivity analysis of fMRI data reveals complex modulation of brain networks. Hum Brain Mapp, 38(11), 5726-5739.

Geva, S., Jones, P. S., Crinion, J. T., Price, C. J., Baron, J. C., & Warburton, E. A. (2011). The neural correlates of inner speech defined by voxel-based lesion-symptom mapping. Brain, 134(Pt 10), 3071-3082.

Grindrod, C. M., & Baum, S. R. (2003). Sensitivity to local sentence context information in lexical ambiguity resolution: Evidence from left- and right-hemisphere-damaged individuals. Brain and Language, 85(3), 503-523.

Guimera, R., & Amaral, L. A. N. (2005). Functional cartography of complex metabolic networks. nature, 433(7028), 895.

Hervé, P. Y., Razafimandimby, A., Vigneau, M., Mazoyer, B., & Tzourio-Mazoyer, N. (2012). Disentangling the brain networks supporting affective speech comprehension. Neuroimage, 61(4), 1255-1267.

Hurschler, M. A., Liem, F., Jäncke, L., & Meyer, M. (2013). Right and left perisylvian cortex and left inferior frontal cortex mediate sentence-level rhyme detection in spoken language as revealed by sparse fMRI. Hum Brain Mapp, 34(12), 3182-3192.
J ankowski, M. M., Ronnqvist, K. C., Tsanov, M., Vann, S. D., Wright, N. F., Erichsen, J. T., . . . O'Mara, S. M. (2013). The anterior thalamus provides a subcortical circuit supporting memory and spatial navigation. Front Syst Neurosci, 7, 45.

Jobard, G., Vigneau, M., Mazoyer, B., & Tzourio-Mazoyer, N. (2007). Impact of modality and linguistic complexity during reading and listening tasks. Neuroimage, 34(2), 784-800.

Joliot, M., Jobard, G., Naveau, M., Delcroix, N., & Petit…, L. (2015). AICHA: An atlas of intrinsic connectivity of homotopic areas. Journal of neuroscience Methods 254:46–59.

Joliot, M., Tzourio-Mazoyer, N., & Mazoyer, B. (2016). Intra-hemispheric intrinsic connectivity asymmetry and its relationships with handedness and language Lateralization. Neuropsychologia, 93(Pt B), 437-447.

Klingbeil, J., Wawrzyniak, M., Stockert, A., & Saur, D. (2017). Resting-state functional connectivity: An emerging method for the study of language networks in post-stroke aphasia. Brain Cogn.

Klostermann, F., Krugel, L. K., & Ehlen, F. (2013). Functional roles of the thalamus for language capacities. Front Syst Neurosci, 7, 32.

Kreisler, A., Godefroy, O., Delmaire, C., Debachy, B., Leclercq, M., Pruvo, J.-P., & Leys, D. (2000). The anatomy of aphasia revisited. Neurology, 54(5), 1117-1123.

Liang, X., Zou, Q., He, Y., & Yang, Y. (2013). Coupling of functional connectivity and regional cerebral blood flow reveals a physiological basis for network hubs of the human brain. Proc Natl Acad Sci U S A, 110(5), 1929-1934.

Liu, H., Stufflebeam, S. M., Sepulcre, J., Hedden, T., & Buckner, R. L. (2009). Evidence from intrinsic activity that asymmetry of the human brain is controlled by multiple factors. Proceedings of the National Academy of Sciences, 106(48), 20499-20503.

Mazoyer, B., Mellet, E., Perchey, G., Zago, L., Crivello, F., Jobard, G., . . . Tzourio-Mazoyer, N. (2016). BIL&GIN: A neuroimaging, cognitive, behavioral, and genetic database for the study of human brain lateralization. Neuroimage, 124(Pt B), 1225-1231.

Mazoyer, B., Zago, L., Jobard, G., Crivello, F., Joliot, M., Perchey, G., . . . Tzourio-Mazoyer, N. (2014). Gaussian mixture modeling of hemispheric lateralization for language in a large sample of healthy individuals balanced for handedness. PLoS One, 9(6), e101165.

Mazoyer, B., Zago, L., Mellet, E., Bricogne, S., & Etard…, O. (2001). Cortical networks for working memory and executive functions sustain the conscious resting state in man. Brain research ….

Mesulam, M., Weintraub, S., Parrish, T., & Gitelman, D. (2005). Primary progressive aphasia: reversed asymmetry of atrophy and right hemisphere language dominance. Neurology, 64(3), 556-557.

Mesulam, M.-M. (1998). From sensation to cognition. Brain: a journal of neurology, 121(6), 1013-1052.

Mesulam, M. M., Rogalski, E. J., Wieneke, C., Hurley, R. S., Geula, C., Bigio, E. H., . . . Weintraub, S. (2014). Primary progressive aphasia and the evolving neurology of the language network. Nat Rev Neurol, 10, 554-569.

Monchi, O., Petrides, M., Strafella, A. P., Worsley, K. J., & Doyon, J. (2006). Functional role of the basal ganglia in the planning and execution of actions. Ann Neurol, 59(2), 257-264.

Nobre, A. C., Allison, T., & McCarthy, G. (1994). Word recognition in the human inferior temporal lobe. Nature, 372(6503), 260.

Ogar, J., Willock, S., Baldo, J., Wilkins, D., Ludy, C., & Dronkers, N. (2006). Clinical and anatomical correlates of apraxia of speech. Brain Lang, 97(3), 343-350.

Ojemann, G., Ojemann, J., Lettich, E. R. E. E. G. T., & Berger, M. (1989). Cortical language localization in left, dominant hemisphere: an electrical stimulation mapping investigation in 117 patients. Journal of neurosurgery, 71(3), 316-326.

Opsahl, T., Agneessens, F., & Skvoretz, J. (2010). Node centrality in weighted networks: Generalizing degree and shortest paths. Social Networks, 32(3), 245-251.

Papathanassiou, D., Etard, O., Mellet, E., Zago, L., Mazoyer, B., & Tzourio-Mazoyer, N. (2000). A common language network for comprehension and production: a contribution to the definition of language epicenters with PET. Neuroimage, 11(4), 347-357.

Pillay, S. B., Binder, J. R., Humphries, C., Gross, W. L., & Book, D. S. (2017). Lesion localization of speech comprehension deficits in chronic aphasia. Neurology, 88(10), 970-975.

Price, A. R., Peelle, J. E., Bonner, M. F., Grossman, M., & Hamilton, R. H. (2016). Causal Evidence for a Mechanism of Semantic Integration in the Angular Gyrus as Revealed by High-Definition Transcranial Direct Current Stimulation. J Neurosci, 36(13), 3829-3838.

Price, C. J. (2000). The anatomy of language: contributions from functional neuroimaging. The Journal of Anatomy, 197(3), 335-359.

Price, C. J. (2010). The anatomy of language: a review of 100 fMRI studies published in 2009. Ann N Y Acad Sci, 1191, 62-88.

Price, C. J. (2012). A review and synthesis of the first 20 years of PET and fMRI studies of heard speech, spoken language and reading. Neuroimage, 62(2), 816-847.

Raichle, M. E. (2015). The restless brain: how intrinsic activity organizes brain function. Philos Trans R Soc Lond B Biol Sci, 370(1668).

Raichle, M. E., & Mintun, M. A. (2006). Brain work and brain imaging. Annu Rev Neurosci, 29, 449-476.

Rauschecker, J. P., & Scott, S. K. (2009). Maps and streams in the auditory cortex: nonhuman primates illuminate human speech processing. Nat Neurosci, 12(6), 718-724.

Richardson, J. D., Fillmore, P., Rorden, C., Lapointe, L. L., & Fridriksson, J. (2012). Re-establishing Broca's initial findings. Brain Lang, 123(2), 125-130.

Rubinov, M., & Sporns, O. (2010). Complex network measures of brain connectivity: uses and interpretations. Neuroimage, 52(3), 1059-1069.

Saur, D., Lange, R., Baumgaertner, A., Schraknepper, V., Willmes, K., Rijntjes, M., & Weiller, C. (2006). Dynamics of language reorganization after stroke. Brain, 129(Pt 6), 1371-1384.

Saur, D., Kreher, B. W., Schnell, S., Kümmerer, D., Kellmeyer, P., Vry, M.-S., . . . Abel, S. (2008). Ventral and dorsal pathways for language. Proceedings of the national academy of Sciences, 105(46), 18035-18040.

Saygin, A. P., Wilson, S. M., Dronkers, N. F., & Bates, E. (2004). Action comprehension in aphasia: linguistic and non-linguistic deficits and their lesion correlates. Neuropsychologia, 42(13), 1788-1804.

Sefcsik, T., Nemeth, D., Janacsek, K., Hoffmann, I., Scialabba, J., Klivenyi, P., . . . Vecsei, L. (2009). The role of the putamen in cognitive functions — A case study. Learning & Perception, 1(2), 215-227.

Sidtis, J. J. (2007). Some problems for representations of brain organization based on activation in functional imaging. Brain Lang, 102(2), 130-140.

Sporns, O., Honey, C. J., & Kötter, R. (2007). Identification and classification of hubs in brain networks. PLoS One, 2(10), e1049.

Spreng, R. N., Mar, R. A., & Kim, A. S. N. (2009). The common neural basis of autobiographical memory, prospection, navigation, theory of mind, and the default mode: a quantitative meta-analysis. Journal of cognitive neuroscience, 21(3), 489-510.

Suzuki, R., & Shimodaira, H. (2004). An application of multiscale bootstrap resampling to hierarchical clustering of microarray data: How accurate are these clusters. The Fifteenth International Conference on ….

Suzuki, R., & Shimodaira, H. (2006). Pvclust: an R package for assessing the uncertainty in hierarchical clustering. Bioinformatics, 22(12), 1540-1542.

Tate, M. C., Herbet, G., Moritz-Gasser, S., Tate, J. E., & Duffau, H. (2014). Probabilistic map of critical functional regions of the human cerebral cortex: Broca's area revisited. Brain, 137(Pt 10), 2773-2782.

Tate, M. C., Herbet, G., Moritz-Gasser, S., Tate, J. E., & Duffau, H. (2015). Reply: probabilistic map of language regions: challenge and implication. Brain, 138(Pt 3), e338.

Tetzloff, K. A., Duffy, J. R., Clark, H. M., Strand, E. A., Machulda, M. M., Schwarz, C. G., . . . Whitwell, J. L. (2018). Longitudinal structural and molecular neuroimaging in agrammatic primary progressive aphasia. Brain, 141(1), 302-317.

Thirion, B., Varoquaux, G., & Dohmatob…, E. (2014). Which fMRI clustering gives good brain parcellations. Frontiers in ….

Thompson, P. M., Andreassen, O. A., Arias-Vasquez, A., Bearden, C. E., Boedhoe, P. S., Brouwer, R. M., . . . ENIGMA, C. (2017). ENIGMA and the individual: Predicting factors that affect the brain in 35 countries worldwide. Neuroimage, 145(Pt B), 389-408.

Tomasi, D., & Volkow, N. D. (2012). Resting functional connectivity of language networks: characterization and reproducibility. Mol Psychiatry, 17(8), 841-854.

Turken, A. U., & Dronkers, N. F. (2011). The neural architecture of the language comprehension network: converging evidence from lesion and connectivity analyses. Front Syst Neurosci, 5, 1.

Tzourio-Mazoyer, N., Joliot, M., Marie, D., & Mazoyer, B. (2016). Variation in homotopic areas' activity and inter-hemispheric intrinsic connectivity with type of language lateralization: an FMRI study of covert sentence generation in 297 healthy volunteers. Brain Struct Funct, 221(5), 2735-2753.

van den Heuvel, M. P., Mandl, R. C., Stam, C. J., Kahn, R. S., & Hulshoff Pol, H. E. (2010). Aberrant frontal and temporal complex network structure in schizophrenia: a graph theoretical analysis. J Neurosci, 30(47), 15915-15926.

van den Heuvel, M. P., & Sporns, O. (2011). Rich-club organization of the human connectome. J Neurosci, 31(44), 15775-15786.

Vigneau, M., Beaucousin, V., Hervé, P. Y., Duffau, H., Crivello, F., Houdé, O., . . . Tzourio-Mazoyer, N. (2006). Meta-analyzing left hemisphere language areas: phonology, semantics, and sentence processing. Neuroimage, 30(4), 1414-1432.

Viñas-Guasch, N., & Wu, Y. J. (2017). The role of the putamen in language: a meta-analytic connectivity modeling study. Brain Struct Funct, 222(9), 3991-4004.

Wada, J., & Rasmussen, T. (1960). Intracarotid injection of sodium amytal for the lateralization of cerebral speech dominance: experimental and clinical observations. Journal of Neurosurgery, 17(2), 266-282.

Wang, D., Buckner, R. L., & Liu, H. (2014). Functional specialization in the human brain estimated by intrinsic hemispheric interaction. J Neurosci, 34(37), 12341-12352.

Wang, J., Xie, S., Guo, X., Becker, B., Fox, P. T., Eickhoff, S. B., & Jiang, T. (2017). Correspondent Functional Topography of the Human Left Inferior Parietal Lobule at Rest and Under Task Revealed Using Resting-State fMRI and Coactivation Based Parcellation. Hum Brain Mapp, 38(3), 1659-1675.

Wig, G. S. (2017). Segregated Systems of Human Brain Networks. Trends in cognitive sciences.

Wilson, S. M., Dronkers, N. F., Ogar, J. M., Jang, J., Growdon, M. E., Agosta, F., . . . Gorno-Tempini, M. L. (2010). Neural correlates of syntactic processing in the nonfluent variant of primary progressive aphasia. J Neurosci, 30(50), 16845-16854.

Yourganov, G., Smith, K. G., Fridriksson, J., & Rorden, C. (2015). Predicting aphasia type from brain damage measured with structural MRI. Cortex, 73, 203-215.

Zago, L., Hervé, P. Y., Genuer, R., Laurent, A., Mazoyer, B., Tzourio-Mazoyer, N., & Joliot, M. (2017). Predicting hemispheric dominance for language production in healthy individuals using support vector machine. Hum Brain Mapp, 38(12), 5871-5889.

Zago, L., Petit, L., Turbelin, M. R., Andersson, F., Vigneau, M., & Tzourio-Mazoyer, N. (2008). How verbal and spatial manipulation networks contribute to calculation: an fMRI study. Neuropsychologia, 46(9), 2403-2414.

Zago, L., & Tzourio-Mazoyer, N. (2002). Distinguishing visuospatial working memory and complex mental calculation areas within the parietal lobes. Neuroscience letters, 331(1), 45-49.